Progress in Favré-Reynolds Stress Closures for Compressible Flows

V. Adumitroaie
State University of New York at Buffalo, Buffalo, New York

J.R. Ristorcelli
ICASE, Hampton, Virginia

D.B. Taulbee
State University of New York at Buffalo, Buffalo, New York

Institute for Computer Applications in Science and Engineering
NASA Langley Research Center
Hampton, VA
Operated by Universities Space Research Association

National Aeronautics and
Space Administration

Langley Research Center
Hampton, Virginia 23681-2199

June 1998

PROGRESS IN FAVRÉ-REYNOLDS STRESS CLOSURES FOR COMPRESSIBLE FLOWS

V. ADUMITROAIE[*], J.R. RISTORCELLI[†], AND D.B. TAULBEE[‡]

Abstract. A closure for the compressible portion of the pressure-strain covariance is developed. It is shown that, within the context of a pressure-strain closure assumption linear in the Reynolds stresses, an expression for the pressure-dilatation can be used to construct a representation for the pressure-strain. Additional closures for the unclosed terms in the Favré-Reynolds stress equations involving the mean acceleration are also constructed. The closures accommodate compressibility corrections depending on the magnitude of the turbulent Mach number, the mean density gradient, the mean pressure gradient, the mean dilatation, and, of course, the mean velocity gradients. The effects of the compressibility corrections are consistent with current DNS results. Using the compressible pressure-strain and mean acceleration closures in the Favré-Reynolds stress equations an algebraic closure for the Favré-Reynolds stresses is constructed. Noteworthy is the fact that, *in the absence of mean velocity gradients*, the mean density gradient produces Favré-Reynolds stresses in accelerating mean flows. Computations of the mixing layer using the compressible closures developed are described. Full Reynolds stress closure and two-equation algebraic models are compared to laboratory data. The mixing layer configuration computations are compared to laboratory data; since the laboratory data for the turbulence stresses is inconsistent, this comparison is inconclusive. Comparisons for the spread rate reduction indicate a sizable decrease in the mixing layer growth rate.

Keywords: compressible turbulence, compressible pressure-strain, algebraic Reynolds stress models

Subject classification: Fluid Mechanics

1. Introduction. There has been a resurgence of interest in effects of compressibility on turbulent flows related to the design of high-speed/high-altitude engines. Although experimental and numerical information is growing (for reviews see [1, 2, 3]) rational theoretical and modeling efforts are in a preliminary stage of development. This is consistent with the fact that what is understood of the relative importance of many of the different physical effects of compressibility is very much in flux — changing as more numerical simulation information becomes available. While several issues regarding the effects of the compressibility of the turbulent fluctuations have been recognized, progress in incorporating the physics responsible for these new compressibility effects in single-point turbulence closures has been slow. One of the major impediments to progress has been the absence of a procedure that would allow for the inclusion of the effects of compressibility on the pressure-strain covariance appearing in the second-order moment equations. A method of including compressibility effects as they appear in the pressure-strain covariance and also the variable inertia effects are the subject of the present study.

---

[*]Department of Mechanical and Aerospace Engineering, State University of New York at Buffalo, Buffalo, NY 14260-4400. Present affiliation: CFD Research Corporation, 215 Wynn Drive, Huntsville, AL 35805.

[†]A portion of this research was supported by the National Aeronautics and Space Administration under NASA Contract No. NAS1-19480 while the second author was in residence at the Institute for Computer Applications in Science and Engineering (ICASE), NASA Langley Research Center, Hampton, VA 23681-0001.

[‡]Department of Mechanical and Aerospace Engineering State University of New York at Buffalo, Buffalo,NY 14260-4400.

Several earlier studies have obtained closures for diverse effects of compressibility. Researchers have, in general, exploited a decomposition of the compressible field into solenoidal and dilatational parts. This has been done using a dimensional analysis in physical space [4] or in Fourier space [5], asymptotic analysis [6], rapid-distortion theory [7], and a singular perturbation method [8]. All these approaches have generated models for new compressible scalar terms, the pressure-dilatation and the dilatational dissipation, that appear in the kinetic energy equation for high-speed flows. Such an approach to compressible turbulence modeling has been called, very sensibly, an "energetic" approach to the effects of compressibility, Simone *et al.* [9]. The models resulting from the "energetic" approach to compressibility have been applied as compressibility corrections to the standard $k - \epsilon$ model, [10], and their generalizations, [5], or to standard incompressible second-order moment [Reynolds stress] closures [11, 12, 13]. Such a procedure is, of course, an implicit statement that compressible effects do not manifest themselves in either the pressure-strain or in the dissipation of enstrophy; the effects of compressibility occur only in those terms explicitly linked to the new terms involving the dilatational field. Thus, energetic approaches to the problem of compressible turbulence, as pointed out in [9], are incomplete.

At one time, the pressure-dilatation and the compressible dissipation, on which modeling effort has been expended, were believed to be the primary physical effects contributing to the reduced growth rate of the compressible mixing layer. Recent studies [14, 15] have demonstrated that the dilatational effects on the mixing layer are, in fact, much smaller than once believed. In addition, more recent direct numerical simulations (DNS) suggest that the pressure-dilatation covariance is nominally more important than the compressible dissipation, contrary to early proposals, [4, 6]. The pressure-dilatation does not, however, account for the reduced growth of the mixing layer. It appears, as suggested in [16], that the phenomena responsible for the reduced growth rate of the turbulent shear flows is due to the reduction in the Reynolds shear stress anisotropy; this effect is thought to be due to the effects of compressibility on the pressure-strain covariance. This viewpoint is consistent with the earlier numerical studies of [17]. The articles [13] and the later [18] studied Reynolds stress closures in the context of the DNS of the homogeneous shear. The study showed that the inclusion of the [then] current compressible dissipation and pressure-dilatation models in the Reynolds stress turbulence closures led to improved predictions for the turbulent kinetic energy. However, there were no changes in the anisotropy consistent with that seen in DNS. The authors concluded that the [then] current models were deficient primarily in the modeling of the pressure-strain covariance which controls the level of Reynolds stress anisotropy.

It should be noted that the improved agreement for the time evolution of the kinetic energy, [13, 18], when using the compressible models of that time cannot be taken to indicate that such flows were rationally predicted. The models current at that time, designed with erroneous assumptions regarding the importance of the dilatational effects, were providing the right amount of dissipation but by mechanisms that did not reflect actual flow physics. This has since been substantiated numerically in the studies [9, 14, 15, 16]; all of which indicate the lack of significance of both the pressure-dilatation and the compressible dissipation. The fact that the compressible dissipation and the pressure-dilatation are nominal effects is also consistent with the analytical development of [8]. In [8] the pressure-dilatation is shown to vanish as turbulence approaches equilibrium; the simulations mentioned are quasi-equilibrium flows. It should be mentioned that in the homogeneous shear simulations, arguably the most non-equilibrium of the benchmark flows, the pressure-dilatation is small but non-negligible; it is some 5-10% of the dissipation. Our position is the same as the position of Vreman *et al.* [14] as pithily summarized in their conclusion; to paraphrase, turbulence

models constructed using the dilatational dissipation or pressure-dilatation to explain the suppression of the turbulence [in the mixing layer] do not appear to be reflecting the correct physics.

Thus, if it is assumed that the primary source of the reduced mixing rate in the mixing layer is due to the reduction in the shear stress anisotropy as indicated by DNS then a closure of the second-moment or Reynolds stress equations is required: the pressure-strain covariance appearing in the second-moment equations is the only possible mechanism for such behavior. This is a substantially more difficult problem than that treated using the energetic approach; the quantities requiring closure are no longer scalars but second-order tensors. As one might expect, true compressible second-order modeling attempts are few, [7, 19].

This article describes the development of a closure for the compressible aspects of pressure-strain covariance appearing in the Favré-Reynolds stress equations. [As is clear from the material, the phrase Reynolds stresses will be used to refer to the Favré-Reynolds stresses.] Closures for the unclosed terms involving the mean acceleration are also constructed. In as much as most engineering calculations [in this country] are done with lower order closures this article therefore also includes the additional development of the second-order moment closure into an algebraic Reynolds stress closure, suitable for flows in structural equilibrium, following established procedures [20, 21, 22, 23, 24, 25, 26, 27, 28].

The algebraic Reynolds stress expression is noteworthy for the fact that it indicates that, even in the absence of mean deformation, the mean density gradient is a source of turbulence stresses in accelerating mean flows. As a consequence, for flows with large arbitrary mean density and pressure gradients an eddy viscosity representation for the Reynolds stresses is, from first principles, inappropriate. Qualifications regarding this statement are further discussed in §4.

In the next section, §2, the Favré averaged nondimensional form of the governing equations are given. Both first and second-order moment equations for a compressible medium, with no combustion, are given. Issues related to moment closures for compressible turbulence are also outlined.

The development of closures for the effects of compressibility in the Reynolds stress equations is described in §3. It is shown that, within the context of a pressure-strain closure *linear* in the Reynolds stresses, an expression for the pressure-dilatation covariance can be used to construct the off-diagonal components of the pressure-strain covariance. In this way the results of previous so-called energetic approaches, [9], to the effects of compressibility can be built into the deviatoric portion of an expression for the pressure-strain. It is hoped that such a procedure would allow one to avoid the development of a whole new theory and methodology for a compressible pressure-strain closure.

Closures for the effects of the mean acceleration, which involve the mass flux, are also developed. The new closures account for the influence of the turbulent Mach number, and the mean density and pressure gradients through a new quantity, the baroclinic dyad. The effects of the bulk dilatation are also included. Section 3 is concluded with a summary of models for the compressible dissipation; given the acknowledged lack of importance of the compressible dissipation in weakly compressible aerodynamic turbulence, as discussed above and in §3, no development of models for the compressible dissipation is pursued.

Starting with the closure for the second-order moment equations developed in §3, §4 develops an algebraic closure for the Reynolds stresses. The physics of compressibility as captured by the full second-moment closure are therefore built into the simpler and more widely used two-equation $k - \epsilon$ platform. The tensor polynomial representation techniques employed produce both two-dimensional and three-dimensional versions of an

algebraic turbulence stress closure. Given the complexity of the three-dimensional algebraic closure and the current status of single-point turbulence models for three-dimensional flow only the two-dimensional model is developed into a working closure.

Section 5 focuses on a numerical investigation of the closures. The numerical method used to simulate the free-shear flows of interest is sketched. The theory and results presented in earlier sections are implemented in simulations in the mixing layer.

Simulations using second-order moment (SOM) closures as well as the algebraic models are conducted. The numerical experiments are constructed with the intention of investigating several very different issues of relevance to the prediction of compressible turbulent flows for engineering purposes. Foremost in importance is the ability of an algebraic stress model - that includes the effects of compressibility - to reflect the physics in the full SOM closures.

The pressure-strain methodology developed for the SOM equations in §3 are general and depend on a choice of closures for the pressure-dilatation. As consequence it follows that it is necessary to understand sensitivity of the formulation to different models for the pressure-dilatation. In this context two pressure-dilatation models are investigated.

In addition to assessing the sensitivity of the pressure-strain model to different pressure-dilatation models and the suitability of the algebraic stress closure, we compare the computational results to what is seen in numerical and laboratory experiments. Of particular interest is the well known effect of compressibility on reduction of the spread rate of the mixing layer. In as much as the reduction in the spread rate is due to changes in the the anisotropy of the Reynolds stresses, as a function of compressibility, are also investigated. Given that the anisotropy of the Reynolds stresses is dependent on the pressure-strain, the effects of compressibility on the different components of the pressure-strain are also investigated.

2. Governing equations. The problem formulation is now described. This includes a statement of the governing equations – the first and second-moment equations. Indications of the modeling issues to be addressed in subsequent sections are also given. The Favré averaging procedure is first described.

The conservation equations for mass, momentum and energy in a Favré setting are now derived. The dependent variables used are the density ρ, the velocity u_i and the total energy $e_t = h - p/\rho + u_i u_i/2$. The fluid is assumed to be Newtonian fluid satisfying the Stokes relation with zero bulk viscosity and a constant molecular Prandtl number. Although real gas effects are of interest for industrial applications there are a sufficient number of unresolved and more important issues associated with compressibility that justify limiting the study to ideal gases. Consequently, the pressure p is obtained from the equation of state $p = \rho R T$.

The Favré averaging procedure is now described: denote by an over-bar the ensemble (or time) average and by the brackets the density weighted ensemble (or time) average:

$$(1) \qquad \langle X \rangle = \frac{\overline{\rho X}}{\overline{\rho}}$$

The ensemble average obeys the following decomposition rules:

$$(2) \qquad X = \overline{X} + X', \quad \overline{X'} = 0.$$

The Favré average obeys the following decomposition rules:

$$(3) \qquad X = \langle X \rangle + X'', \quad \langle X'' \rangle = 0, \quad \overline{X''} = \overline{X} - \langle X \rangle.$$

The application of the above averaging procedure on the instantaneous transport equations, decomposing the variables Favré mean and fluctuating components, produces the Favré averaged equations. The equations of motion are first rewritten in nondimensional form (with respect to reference values taken in the high speed stream: ρ_∞, u_∞, T_∞, μ_∞ and the inlet value of the vorticity thickness δ_ω). Using these reference quantities, we define the relevant nondimensional parameters: the Reynolds number $Re = \rho_\infty u_\infty \delta_\omega / \mu_\infty$, the Prandtl number $Pr = c_p \mu_\infty / \lambda$, the mean flow Mach number $M = u_\infty / \sqrt{\gamma R T_\infty}$, γ is c_p / c_v. For this study, $Pr = 1$.

2.1. First moment equations. The mass conservation equation reads:

$$(4) \qquad \frac{\partial \overline{\rho}}{\partial t} + \frac{\partial \overline{\rho} \langle u_j \rangle}{\partial x_j} = 0$$

and the conservation of momentum is:

$$(5) \qquad \frac{\partial \overline{\rho} \langle u_i \rangle}{\partial t} + \frac{\partial \overline{\rho} \langle u_i \rangle \langle u_j \rangle}{\partial x_j} = -\frac{\partial \overline{\rho} \langle u_i'' u_j'' \rangle}{\partial x_j} - \frac{\partial \overline{p}}{\partial x_i} + \frac{\partial \overline{\sigma}_{ji}(u)}{\partial x_j}.$$

Note that the stress tensor notation is changed to $\sigma_{ji}(u) = \frac{2\mu}{Re}[S_{ij}(u) - \frac{1}{3}S_{pp}(u)\delta_{ij}] = 2\mu S_{ij}^\star(u)/Re$. For the strain rate $S_{ij}(u) = \frac{1}{2}(\frac{\partial u_i}{\partial x_j} + \frac{\partial u_j}{\partial x_i})$ and for all the other linear differential operators, this new notation is more suitable when investigating compressible flows. In these instances the two types of averages, having different properties with respect to the linear differential operators, are naturally encountered. Hereafter any tensor with a star superscript will indicate the deviator – the traceless portion of that tensor.

Two supplementary hypotheses pertaining to the molecular transport of momentum are set forth: the viscosity fluctuations are unimportant and the mean viscosity $\langle \mu \rangle$ is described by the Maxwell-Rayleigh law, i.e., it varies with the mean temperature as $\langle \mu \rangle / \mu_{ref} = (\langle T \rangle / T_{ref})^m$, $m = 0.76$. The fluctuations of the viscosity and their correlation with other variables are neglected. Within the current notation the averaged stress $\overline{\sigma}_{ji}(u)$ is equal to $\sigma_{ji}(\langle u \rangle) + \sigma_{ji}(\overline{u''})$.

The Favré mean of the total energy of the fluid $e_t = T/[\gamma(\gamma - 1)M^2] + u_j u_j / 2$ obeys:

$$(6) \qquad \frac{\partial \overline{\rho} \langle e_t \rangle}{\partial t} + \frac{\partial \overline{\rho} \langle e_t \rangle \langle u_j \rangle}{\partial x_j} = -\frac{\partial \overline{q}_j(T)}{\partial x_j} - \frac{\partial \overline{\rho} \langle u_j'' e_t'' \rangle}{\partial x_j} + \frac{\partial}{\partial x_j}(\overline{u_i \sigma}_{ji}(u) - \overline{p u_j}).$$

As is the situation with the momentum equation, the molecular flux term in the energy equation introduces the other type of mean quantity present in the Favré formulation - the plain ensemble mean. Using the new notation, the heat flux

$$q_j(T) = -\frac{\mu}{(\gamma - 1)Re Pr M^2} \frac{\partial T}{\partial x_j}$$

has the resulting averaged expression:

$$\overline{q}_j(T) = q_j(\langle T \rangle) + q_j(\overline{T''}).$$

The remaining terms on the right-hand side of the energy equation can be expanded by using the equation of state in the average sense

$$(7) \qquad \overline{p} = \frac{1}{\gamma M^2} \overline{\rho} \langle T \rangle.$$

Then the pressure work term is of the form

$$\overline{pu_j} = \overline{p}\langle u_j \rangle + \frac{1}{\gamma M^2}\overline{p}\langle u_j'' T'' \rangle,$$

the viscous work term reads

$$\overline{u_i \sigma}_{ji}(u) = \langle u_i \rangle \sigma_{ji}(\langle u \rangle) + \langle u_i \rangle \sigma_{ji}(\overline{u''}) + \overline{u''}\sigma_{ji}(\langle u \rangle) + \overline{u''_i \sigma}_{ji}(u'')$$

and the turbulent total energy flux is

$$\overline{\rho}\langle u_j'' e_t'' \rangle = \frac{1}{\gamma(\gamma-1)M^2}\overline{\rho}\langle u_j'' T'' \rangle + \overline{\rho}\langle u_j'' u_i'' \rangle\langle u_i \rangle + \overline{\rho}\frac{\langle u_j'' u_i'' u_i'' \rangle}{2}.$$

The fluctuations of transported quantities in turbulent flows are sustained via interaction between the mean gradients and the turbulence. The fluctuations will be characterized by length and time scales of the order of those of the mean flow and which, provided the Reynolds number is large, will be many orders of magnitude larger than the fine scales at which the molecular diffusion is important. Thus the form of the moment equations carried in the closure development for the computation of free shear flows will not include viscous transport effects.

2.2. Second-order moment equations. The average of the first moment of the Favré decomposed Navier-Stokes equations produces the following second moment equations:

$$\frac{\partial \overline{\rho}\langle u_i'' u_j'' \rangle}{\partial t} + \frac{\partial \overline{\rho}\langle u_i'' u_j'' \rangle\langle u_k \rangle}{\partial x_k} = -\frac{\partial}{\partial x_k}\left[\overline{\rho}\langle u_i'' u_j'' u_k'' \rangle + \overline{p' u_j''}\delta_{ik} + \overline{p' u_i''}\delta_{jk} - \overline{u_i'' \sigma_{kj}(u'')} - \right.$$

$$\left. \overline{u_j'' \sigma_{ki}(u'')}\right] - \overline{\rho}\langle u_i'' u_k'' \rangle\frac{\partial \langle u_j \rangle}{\partial x_k} - \overline{\rho}\langle u_k'' u_j'' \rangle\frac{\partial \langle u_i \rangle}{\partial x_k} + \overline{p'\left(\frac{\partial u_i''}{\partial x_j} + \frac{\partial u_j''}{\partial x_i}\right)} - \overline{u_i''}\frac{\partial \overline{p}}{\partial x_j} - \overline{u_j''}\frac{\partial \overline{p}}{\partial x_i}$$

(8)
$$+\overline{u_j''}\frac{\partial \sigma_{ki}(\langle u \rangle)}{\partial x_k} + \overline{u_i''}\frac{\partial \sigma_{kj}(\langle u \rangle)}{\partial x_k} - \left[\overline{\sigma_{jk}(u'')\frac{\partial u_i''}{\partial x_k}} + \overline{\sigma_{ki}(u'')\frac{\partial u_j''}{\partial x_k}}\right]$$

It is necessary to provide a closure for two compressible quantities: the pressure-strain correlation and the mass flux/pressure gradient (the last three terms in the second line). The molecular diffusion terms are generally small in high Reynolds number flows and will be negligible for problems addressed here. It should be pointed out that, depending on how the derivation is done, the mass flux terms multiply the acceleration of the mean flow. For this reason the mass flux terms are often called acceleration terms: they appear to be important in accelerating mean flows.

Various tensors are divided into their traces and their deviators. The production of the Reynolds stresses becomes,

(9)
$$P_{ij}^\star = P_{ij} - \frac{2}{3}P\delta_{ij} = -\overline{\rho}\left[\langle u_i'' u_k'' \rangle\frac{\partial \langle u_j \rangle}{\partial x_k} + \langle u_k'' u_j'' \rangle\frac{\partial \langle u_i \rangle}{\partial x_k} - \frac{2}{3}\langle u_k'' u_l'' \rangle\frac{\partial \langle u_l \rangle}{\partial x_k}\delta_{ij}\right]$$

where P is the production of $\langle k \rangle$. The pressure-strain covariance is written as

(10)
$$\Pi_{ij}^\star = \Pi_{ij} - \frac{2}{3}\overline{p'd}\delta_{ij} = \overline{p'\left(\frac{\partial u_i''}{\partial x_j} + \frac{\partial u_j''}{\partial x_i}\right)} - \frac{2}{3}\overline{p'\frac{\partial u_k''}{\partial x_k}}\delta_{ij}.$$

The viscous and pressure acceleration terms are written, respectively, as

(11)
$$\mathcal{V}_{ij}^\star = \mathcal{V}_{ij} - \frac{2}{3}\mathcal{V}\delta_{ij} = \overline{u_j''}\frac{\partial \sigma_{ki}(\langle u \rangle)}{\partial x_k} + \overline{u_i''}\frac{\partial \sigma_{kj}(\langle u \rangle)}{\partial x_k} - \frac{2}{3}\overline{u_l''}\frac{\partial \sigma_{kl}(\langle u \rangle)}{\partial x_k}\delta_{ij}$$

and

(12)
$$\mathcal{M}_{ij}^{\star} = \mathcal{M}_{ij} - \frac{2}{3}\mathcal{M}\delta_{ij} = -\left[\overline{u_i'' \frac{\partial \overline{p}}{\partial x_j}} + \overline{u_j'' \frac{\partial \overline{p}}{\partial x_i}} - \frac{2}{3}\overline{u_k'' \frac{\partial \overline{p}}{\partial x_k}}\delta_{ij}\right].$$

Note that the mean pressure gradient appearing in M_{ij} and the mean viscous stress appearing in $\mathcal{V}_{ij}$ can be replaced using the mean momentum equations. In which case they are written in terms of the mean flow Lagrangian acceleration. Both of these terms involve the mass flux; any closure for these two acceleration terms requires a closure for the mass flux. The dissipation is rewritten as

(13)
$$\overline{\rho}\,\epsilon_{ij}^{\star} = \overline{\rho}\left(\overline{\epsilon}_{ij} - \frac{2}{3}\overline{\epsilon}\delta_{ij}\right) = \overline{\sigma_{jk}(u'')\frac{\partial u_i''}{\partial x_k}} + \overline{\sigma_{ki}(u'')\frac{\partial u_j''}{\partial x_k}} - \frac{2}{3}\overline{\sigma_{lk}(u'')\frac{\partial u_l''}{\partial x_k}}\delta_{ij}$$

In turbulent free shear flows the viscous diffusion part is overlooked owing to high Reynolds numbers which are characteristic to these flows. The present analysis can accommodate the discarded viscous terms when necessary; the tensor $\mathcal{V}_{ij}$ will be carried for generality. Furthermore, the turbulent transport terms are considered together:

(14)
$$T_{ijk} = -\left[\overline{\rho}\langle u_i'' u_j'' u_k''\rangle + \overline{p'u_j''}\delta_{ik} + \overline{p'u_i''}\delta_{jk} - \overline{u_i''\sigma_{kj}(u'')} - \overline{u_j''\sigma_{ki}(u'')}\right].$$

The Reynolds stress or second-order moment equations are then written

$$\frac{\partial\overline{\rho}\langle u_i'' u_j''\rangle}{\partial t} + \frac{\partial\overline{\rho}\langle u_i'' u_j''\rangle\langle u_k\rangle}{\partial x_k} = \frac{\partial}{\partial x_k}T_{ijk} + P_{ij}^{\star} + \Pi_{ij}^{\star} + \mathcal{M}_{ij}^{\star} + \mathcal{V}_{ij}^{\star} - \overline{\rho}\,\epsilon_{ij}^{\star}$$

(15)
$$+\frac{2}{3}\left[P + \overline{p'd} + \mathcal{M} + \mathcal{V} - \overline{\rho}\,\overline{\epsilon}\right]\delta_{ij}$$

The equation for the anisotropy. The single point anisotropy tensor, **a**, is defined

(16)
$$a_{ij} = \langle u_i'' u_j''\rangle/\langle k\rangle - \frac{2}{3}\delta_{ij}.$$

The anisotropy has zero trace. Note that the Reynolds stress has been normalized by $\langle k\rangle$ and not $2\langle k\rangle$; in which case this version of the anisotropy is related to an older definition by $a_{ij} = 2b_{ij}$. The turbulence time scale is $\tau = \langle k\rangle/\overline{\epsilon}_s$ where $\overline{\epsilon}_s$ is the solenoidal dissipation. The second invariants of the mean strain and rotation are denoted by $\sigma^2 = S_{ij}^{\star}(\langle u\rangle)S_{ji}^{\star}(\langle u\rangle)$ and $\omega^2 = \Omega_{ij}(\langle u\rangle)\Omega_{ij}(\langle u\rangle)$.

For subsequent manipulations used to derive an algebraic stress closure in §4 we replace the second-order transport equations with an equation for $\langle k\rangle$ and the anisotropy tensor. The following form of the transport equation for the anisotropy tensor, [21], will be used:

$$\tau\sigma\overline{\rho}\frac{Da_{ij}/(\tau\sigma)}{Dt} = \frac{1}{\langle k\rangle}\left[\frac{\partial T_{ijk}}{\partial x_k} - \frac{\langle u_i'' u_j''\rangle}{\langle k\rangle}\frac{\partial T_k}{\partial x_k}\right] - \frac{a_{ij}}{\langle k\rangle}\left[\frac{\partial T_k}{\partial x_k} - \tau\frac{\partial T_k^{\epsilon}}{\partial x_k}\right]$$

$$+\frac{1}{\langle k\rangle}\left[P_{ij}^{\star} + \Pi_{ij}^{\star} + \mathcal{M}_{ij}^{\star} + \mathcal{V}_{ij}^{\star} - \overline{\rho}\,\epsilon_{ij}^{\star}\right] -$$

(17)
$$\overline{\rho}\frac{a_{ij}}{\tau}\left[C_{\epsilon_2} - 2 + (2 - C_{\epsilon_1})\frac{P}{\overline{\rho}\,\overline{\epsilon}_s} + \frac{\tau}{\sigma}\frac{D\sigma}{Dt} + 2\frac{\mathcal{M} + \mathcal{V} + \overline{p'd} - \overline{\rho}\,\overline{\epsilon}_c}{\overline{\rho}\,\overline{\epsilon}_s}\right]$$

where D/Dt indicates the mean Lagrangian derivative, $D/Dt = \frac{\partial}{\partial t} + \langle u_j\rangle\frac{\partial}{\partial x_j}$.

7

The kinetic energy equation. The equation for the turbulent kinetic energy $\langle k \rangle = \langle u_i'' u_i'' \rangle / 2$ is

$$\frac{\partial \overline{\rho} \langle k \rangle}{\partial t} + \frac{\partial \overline{\rho} \langle k \rangle \langle u_j \rangle}{\partial x_j} = - \frac{\partial}{\partial x_j} \left[\overline{\rho} \langle u_j'' k \rangle + \overline{p' u_j''} - \overline{u_i'' \sigma_{ji}(u'')} \right] - \overline{\rho} \langle u_i'' u_j'' \rangle \frac{\partial \langle u_i \rangle}{\partial x_j}$$

(18)
$$+ \overline{p' \frac{\partial u_i''}{\partial x_i}} - \overline{u_j''} \frac{\partial \overline{p}}{\partial x_j} + \overline{u_j''} \frac{\partial \sigma_{ji}(\langle u \rangle)}{\partial x_j} - \overline{\sigma_{ji}(u'') \frac{\partial u_i''}{\partial x_j}}.$$

The additional terms reflecting the compressible nature of the turbulence are on the last line; they are, respectively, the pressure-dilatation covariance, the mass flux – mean acceleration, and the compressible dissipation. Note that neither the pressure-strain nor the mass flux/pressure acceleration terms, $\mathcal{M}_{ij}$, appear in the $\langle k \rangle$ equation. The effects of the pressure-strain and the $\mathcal{M}_{ij}$, appears only in the Reynolds stress equations. Any classical two-equation turbulence model cannot, as a consequence, account for the physics associated with these two unknown covariances that lead to changes in the Reynolds stress structure. Early approaches accounting for the effects of compressibility have focussed only on the effects of compressibility as they occur in the energy equation. This so-called "energetic" approach, to use the phrase of Simone *et al.* [9], for the effects of compressibility misses the changes in the Reynolds stresses due to compressibility and inertia. It is for this reason that, in §3, the second-order equations are closed. An algebraic Reynolds stress closure is then derived in §4. In this way the structural effects of compressibility, for a certain class of flows, can be accounted for in the context of a two-equation single-point closure.

The dissipation equation. The dissipation appearing in the kinetic energy equation is typically written, for locally homogeneous flows,

(19)
$$\overline{\sigma_{ji}(u'') \frac{\partial u_i''}{\partial x_j}} = \overline{\rho} \, \overline{\epsilon} = \overline{\rho}(\overline{\epsilon}_s + \overline{\epsilon}_c) = 2\overline{\mu \Omega_{ij}(u'') \Omega_{ij}(u'')} + \frac{4}{3} \overline{\mu S_{kk}^2(u'')}$$

[4, 6, 29], with $\Omega_{ij}(u) = \frac{1}{2}(\frac{\partial u_i}{\partial x_j} - \frac{\partial u_j}{\partial x_i})$ as the rotation rate. It is customary to compute the solenoidal dissipation from the incompressible $k - \epsilon$ model extended to variable density flows:

(20)
$$\frac{\partial \overline{\rho} \, \overline{\epsilon}_s}{\partial t} + \frac{\partial \overline{\rho} \, \overline{\epsilon}_s \langle u_j \rangle}{\partial x_j} = - \frac{\partial}{\partial x_j} \left[\overline{\rho} \langle u_j'' \epsilon_s \rangle - \frac{\mu}{Re} \frac{\partial \overline{\epsilon}_s}{\partial x_j} \right] - C_{\epsilon_1} \overline{\rho} \frac{\overline{\epsilon}_s}{\langle k \rangle} \langle u_i'' u_j'' \rangle \frac{\partial \langle u_i \rangle}{\partial x_j} - C_{\epsilon_2} \overline{\rho} \frac{\overline{\epsilon}_s^2}{\langle k \rangle},$$

where $C_{\epsilon_1} = 1.44$ and $C_{\epsilon_2} = 1.92$.

3. Compressible closures for the second-order moment equations. This section describes the development of closures for the unknown terms in the second-order equations. The pressure-strain covariance appearing in the Reynolds stress equations is closed using a linear tensor polynomial representation in the Reynolds stress following well established procedures similar to Launder *et al.* [30]. In recognition of the minor role viscosity plays in high Reynolds number free shear flows, only pressure-strain and pressure-acceleration closures are addressed. The pressure-acceleration terms are closed using a leading order [isotropic] gradient transport expression for the mass flux. The following section, §4, uses the results of the present section to obtain an algebraic closure for the Reynolds stresses.

3.1. A closure for the pressure-strain covariance. In incompressible turbulence the closure of the pressure-strain covariance by a tensor polynomial linear in the Reynolds stresses is used with notable success for simple two-dimensional mean flows. The procedure is standard; a popular early reference is Launder *et al.*[30]. An updated version of the linear [30] rapid pressure-strain modeling is given in Speziale *et al.* [31]. As the ultimate goal is to devise an algebraic Reynolds stress model only pressure-strain models linear

in the Reynolds stresses will be considered. A discussion of nonlinear rapid-pressure-strain model and the need for realizability can be found in [32]. Additional discussion of the physical assumptions underlying such methodologies can be found in [33], [34] and [35].

The compressible correction to the pressure-strain covariance representation is obtained using established linear procedures. As in the incompressible situation, [30, 34, 32], the pressure strain-covariance closure can be written as:

$$(21) \qquad \Pi_{ij} - \overline{\rho}\, \epsilon_{ij}^{\star} = \mathcal{A}_{ij} + 2\overline{\rho}\,[\mathcal{I}_{piqj} + \mathcal{I}_{pjqi}][S_{pq}(\langle u \rangle) + \Omega_{pq}(\langle u \rangle)].$$

Such an expression is possible if the supplementary compressible terms appearing in the Poisson equation for the pressure (see Appendix) are, in the weakly compressible limit, of higher order. This will be the case if the evanescent wave portion of the initial value problem is not important as is the case for aerodynamic applications, [36]. The tensors in the above decomposition are modeled as:

$$(22) \qquad \mathcal{A}_{ij} = -C_1 \overline{\rho}\, \overline{\epsilon} a_{ij} + \mathcal{A}_{pp} \frac{\delta_{ij}}{3}$$

$$\frac{\mathcal{I}_{pjqi}}{\langle k \rangle} = \alpha_1 \delta_{qi}\delta_{pj} + \alpha_2(\delta_{pq}\delta_{ij} + \delta_{qj}\delta_{pi}) + \beta_1 \delta_{pj} a_{qi}$$

$$(23) \qquad + \beta_2(\delta_{pq}a_{ij} + \delta_{pi}a_{qj} + \delta_{ij}a_{pq} + \delta_{jq}a_{pi}) + \beta_3 \delta_{qi} a_{pj}$$

Here $\mathcal{I}_{pjqi}$, following precedent, is linear in the Reynolds stresses satisfying necessary symmetry requirements. There are five unknowns. To determine the coefficients in $\mathcal{I}_{pjqi}$ additional constraints are required. As is the usual procedure, the normalization constraint, [30, 32], requires

$$(24) \qquad \mathcal{I}_{ppqi} = [(3\alpha_1 + 2\alpha_2)\delta_{qi} + (3\beta_1 + 4\beta_2)a_{qi}]\langle k \rangle = \langle u_q'' u_i'' \rangle$$

which can be satisfied if

$$3\alpha_1 + 2\alpha_2 = 2/3$$
$$3\beta_1 + 4\beta_2 = 1.$$

There are now three unknowns and additional information is required to obtain them.

In incompressible turbulence modeling the trace of the pressure-strain is zero, $\mathcal{I}_{pkqk} = 0$, and this provides the additional information to determine the unknowns. In compressible turbulence the trace of the pressure-strain is the pressure-dilatation and the so-called continuity constraint becomes

$$(25) \qquad \mathcal{A}_{kk} + 4\overline{\rho}\, \mathcal{I}_{pkqk}[S_{pq} + \Omega_{pq}] = 2\overline{p'd}.$$

As the right hand side, $\overline{pd}$, is known from earlier energetic approaches to the compressible turbulence modeling problem, the continuity constraint, equation (25), becomes a constraint that determines the coefficients in the pressure-strain closure. Note that as $\overline{pd}$ vanishes with turbulent Mach number the incompressible limit, $\mathcal{A}_{kk} + 4\overline{\rho}\, \mathcal{I}_{pkqk}[S_{pq} + \Omega_{pq}] = 0$, is recovered for vanishing compressibility.

As a consequence of the continuity constraint a certain combination of coefficients appears in the final model. These are readily defined by a portion of (25) such that

$$(26) \qquad \mathcal{I}_{piqi}/\langle k \rangle = (\alpha_1 + 4\alpha_2)\delta_{pq} + (\beta_1 + 5\beta_2 + \beta_3)a_{pq} = d_1\delta_{pq} + d_2 a_{pq}.$$

The final model for the compressible portions of the pressure-strain is then written in terms of d_1 and d_2. The values of d_1 and d_2, as will be indicated shortly, are then determined by the expression for the pressure-dilatation. The values of the α_i can be related to the d_i:

$$\alpha_1 = -d_1/5 + 4/15, \quad \alpha_2 = 3d_1/10 - 1/15$$
$$\beta_1 = (15 + 6C_2)/33, \quad \beta_2 = -(2 + 3C_2)/22$$
$$\beta_3 = d_2 + C_2/2.$$

and $C_3 = (5 - 9C_2)/11$, $C_4 = (1 + 7C_2)/11$.

Application of the normalization and continuity constraints then allows the linear pressure-strain model to be written as

$$\Pi_{ij}^{\star} - \overline{\rho}\,\epsilon_{ij}^{\star} = -C_1\overline{\rho}\,\overline{\epsilon}a_{ij} + \overline{\rho}\langle k\rangle \left[\left(\frac{4}{5} + \frac{2}{5}d_1 \right) S_{ij}^{\star}(\langle u\rangle) + \right.$$

$$[1 - C_3 + 2d_2]\left[a_{ip}S_{pj}^{\star}(\langle u\rangle) + S_{ip}^{\star}(\langle u\rangle)a_{pj} - \frac{2}{3}S_{pq}^{\star}(\langle u\rangle)a_{pq}\delta_{ij} \right] -$$

(27) $$\left. [1 - C_4 - 2d_2][a_{ip}\Omega_{pj}(\langle u\rangle) - \Omega_{ip}(\langle u\rangle)a_{pj}] + \frac{4}{3}d_2 S_{pp}(\langle u\rangle)a_{ij} \right]$$

which follows from (21) after subtracting the pressure-dilatation from the left side and the pressure-dilatation model from the right side of (21). All terms involving the d_i represent corrections due to the compressibility of the fluctuations; the d_i vanish as the turbulent Mach number vanishes. The terms involving the C_i come from the incompressible pressure-strain model. In which case the choice of the C_i allow one's favorite incompressible pressure-strain model to be used. The above expression for the pressure-strain is used in calculations presented in this paper. The calculations in this article are of standard test flows and are very simple flows. In more complex flows realizable issues may need to be incorporated. A realizable form of the model is given in an Appendix; more details can be found in Adumitroaie [37].

3.1.1. Commentary. It has been seen that the knowledge of one invariant of the pressure-strain, the pressure-dilatation, *and* the assumption of a form linear in the Reynolds stress allows one to obtain a model for the deviatoric components of the pressure-strain tensor. In this way an independent new theory for the compressible pressure-strain can be avoided by using the results of developments for the scalar pressure-dilatation. The results of previous so-called energetic approaches, Simone *et al.* [9], to the effects of compressibility is built into the deviatoric portion of an expression for the pressure-strain.

This point merits consideration from another point of view. Consider, for the moment, the following partition of the pressure-strain:

(28) $$\overline{ps_{ij}} = \overline{ps_{ij}^*} + \frac{2}{3}\overline{pd}\delta_{ij}.$$

For this subsection, the primes on p have been dropped. Here by s_{ij}^* we now mean the deviatoric portion of the fluctuating strain, $s_{jj}^* = 0$, which contains solenoidal and compressible contributions $s_{ij}^* = s_{ij}^{*I} + s_{ij}^{*C}$, where, of course, $s_{ij}^{*I} = s_{ij}^I$. This is done for ease of presentation; in the nomenclature of §2 these quantities would, of course, be represented by $S_{ij}^*(u'')$ a precision unnecessary for the present discussion. Thus one can write

(29) $$\overline{ps_{ij}} = \overline{ps_{ij}^*}^I + \overline{ps_{ij}^*}^C + \frac{2}{3}\overline{pd}\,\delta_{ij}.$$

The term $\overline{ps_{ij}^*}^I$ is closed using standard incompressible pressure-strain closures. The pressure-dilatation is closed using models already in the literature, see §3.2 below. In §3.1 an expression for $\overline{ps_{ij}^{*C}}$ has been obtained.

As has already been discussed in energetic approaches, the pressure-dilatation cannot account for the suppression of the turbulence by the reduction in the shear stress as is seen in compressible flows. A straightforward extension of the energetic approach to the second-order closure level implies

$$(30) \qquad \overline{ps_{ij}} = \overline{ps_{ij}^*}^I + \frac{2}{3}\overline{pd}\,\delta_{ij}.$$

Such an expression, as is consistent with [13, 18], is likewise unsuccessful in reducing the turbulence shear stress. As will be discussed further in §5 the pressure-dilatation is a small quantity and has a nominal effect, for $\alpha \approx 1$, on the turbulence stresses and energy when it is included in the spherical portion of the pressure-strain. Our procedure, using the pressure-dilatation, produces an expression for the compressible contribution to the deviatoric portions of the pressure strain, $\overline{ps_{ij}^*}^C$. In fact, as was born out by computational experiments, had the expression

$$(31) \qquad \overline{ps_{ij}} = \overline{ps_{ij}^*}^I + \overline{ps_{ij}^*}^C$$

[without $\overline{pd}$ on the diagonal] been used in the numerical investigations reported in §5, our results would not have changed much, for $\alpha < 1$.

3.1.2. Pressure-dilatation models. To obtain the final form of the pressure-strain an expression for $\overline{pd}$ is required. There are some choices. Some proposals for $\overline{pd}$ require the solution of transport equations for the density variance [5] or pressure variance [7]. There are two pressure-dilatation models [8, 38] that do not require separate equations. The model of Sarkar [38] is:

$$(32) \qquad \frac{1}{2}\Pi_{pp} = \overline{p'd} = -3\chi_1 M_t^2 [\frac{2}{3}(\frac{1}{\sqrt{3}M_t} - 8\frac{\chi_3}{\chi_1})\overline{\rho}\langle k\rangle S_{pp} + \frac{P}{\sqrt{3}M_t} - \frac{\chi_2}{\chi_1}\overline{\rho}\,\overline{\epsilon}_s]$$

where $\chi_1 = 0.15$, $\chi_2 = 0.2$, and $\chi_3 = 0$ (still to be determined by the author). Note that the model as we have grouped the terms makes it appear as if it is singular in M_t; it is most definitely not singular. The model of Ristorcelli [8] is

$$\overline{p'd} = -\chi M_t^2 [P - \overline{\rho}\,\overline{\epsilon} + T_k - \frac{3}{4}M_t^2\gamma(\gamma - 1)(P_T + \overline{\rho}\,\overline{\epsilon} + T_T)]$$

$$(33) \qquad\qquad -\overline{\rho}\langle k\rangle M_t^2\chi'\frac{D(3\sigma^2 + 5\omega^2)}{Dt}$$

where

$$\chi = \frac{2I_{pd}}{1 + 2I_{pd}M_t^2 + \frac{2}{3}I_{pd}M_t^4\gamma(\gamma-1)}, \quad \chi' = \frac{I_{pd}^r}{1 + 2I_{pd}M_t^2 + \frac{2}{3}I_{pd}M_t^4\gamma(\gamma-1)},$$

$$(34) \qquad I_{pd} = \frac{2}{3}I_1^s + I_{pd}^r\left[3\sigma^2 + 5\omega^2\right], \qquad\qquad I_{pd}^r = \frac{1}{30}\left(\frac{2}{3}\right)^3\alpha^2 I_1^r.$$

Here α is the proportionality constant in the Kolmogorov scaling; we return to this in more detail below. These two models, as well as a third (the Aupoix model), have been discussed in [39].

The d_i are determined by the pressure-dilatation model. For the Sarkar model, one requires that

$$(35) \qquad d_1 = \frac{8\chi_3 M_t^2}{3}, \ d_2 = \frac{\chi_1 M_t}{2}$$

$$(36) \qquad \frac{\mathcal{A}_{pp}}{2} = \chi_2 M_t^2 \overline{\rho} \, \overline{\epsilon}_s.$$

For the Ristorcelli model one requires that

$$(37) \qquad d_1 = \frac{\chi M_t^2}{3}, \ d_2 = \frac{\chi M_t^2}{2}$$

$$(38) \qquad \frac{\mathcal{A}_{pp}}{2} = \chi M_t^2 [\overline{\rho} \, \overline{\epsilon} + \frac{3}{4} M_t^2 \gamma(\gamma - 1)(P_T + \overline{\rho} \, \overline{\epsilon})] - \overline{\rho} \langle k \rangle M_t^2 \chi' \frac{D(3\sigma^2 + 5\omega^2)}{Dt}.$$

Transport terms have been neglected; this is necessary to obtain an algebraic closure [which requires homogeneity]. The compressibility of the turbulence will only be important where the turbulence energy is large [and thus also M_t], which is typically in regions of large production and where transport is not as important. Which is to say that transport is only of importance in the peripheral regions of simple flows – regions where the turbulence intensity is low, production low, and [therefore] the fluctuations are essentially incompressible.

3.2. The mass flux and pressure-acceleration closures. The models for mass fluxes have not undergone much development and their importance in a general flow is not fully understood. Judging from the equations one can infer that the mass flux will be important in accelerating flows with large density gradients. There has been some research on the mass flux: [5] solved its transport equations and Ristorcelli [40] showed how an algebraic model for the mass flux can be obtained from its transport equation:

$$(39) \qquad \overline{\rho} \, \overline{u_i''} = \tau_u \left[\nu_0 \delta_{ij} + \nu_1 \tau_u \frac{\partial \langle u_i \rangle}{\partial x_j} + \nu_2 \tau_u^2 \frac{\partial \langle u_i \rangle}{\partial x_k} \frac{\partial \langle u_k \rangle}{\partial x_j} \right] \langle u_j'' u_p'' \rangle \frac{\partial \overline{\rho}}{\partial x_p}$$

where $\tau_u = M_t \tau / [1 + \frac{M_t \overline{\epsilon}}{2\overline{\epsilon}_s}(P/(\overline{\rho} \, \epsilon) - 1)]$. Here ν_0, ν_1 and ν_2 are the coefficients retrieved from the inversion of the matrix $G_{ij} = \delta_{ij} + \tau_u \frac{\partial \langle u_i \rangle}{\partial x_j}$: $\nu_0 = -(1 + I_\mathbf{G} + II_\mathbf{G})\nu_2$, $\nu_1 = (1 + I_\mathbf{G})\nu_2$, $\nu_2 = (1 + I_\mathbf{G} + II_\mathbf{G} + III_\mathbf{G})^{-1}$, the Roman numbers representing the invariants of $\mathbf{G}$. Note that the leading order term is a gradient transport model. For an isotropic turbulence, an eddy viscosity formulation is possible. For the present set of simple benchmark shear flows, one does not expect the mass flux terms to be very important – the mean flow does not accelerate much. We shall for the sake of simplicity use the eddy viscosity form of the mass flux – the lowest order contribution in the polynomial given above. This is consistent with the gradient transport model used in [11].

The baroclinic dyad, a tensor product formed from the mean density and pressure gradients, is defined as

$$(40) \qquad \mathcal{R}_{ij} = \frac{\partial \overline{p}}{\partial x_i} \frac{\partial \overline{\rho}}{\partial x_j}$$

and the mass flux/acceleration terms in the second-moment equations can then be written, using the leading order portion of 39, as

$$(41) \qquad \mathcal{M}_{ij}^\star = -\frac{1}{\overline{\rho}} \frac{2}{3} \tau_u \nu_0 \langle k \rangle (\mathcal{R}_{ij} + \mathcal{R}_{ji} - \frac{2}{3}\mathcal{R}_{pp}\delta_{ij}) = -\frac{1}{\overline{\rho}} \frac{2}{3} \tau_u \nu_0 \langle k \rangle R_{ij}^\star$$

where $R_{ij}^\star = \mathcal{R}_{ij} + \mathcal{R}_{ji} - \frac{2}{3}\mathcal{R}_{pp}\delta_{ij}$.

3.3. The compressible dissipation. There are several models available for the compressible dissipation, [4, 5, 6, 8]. Many of these models reflect certain assumptions regarding the importance of the compressible dissipation observed in early DNS of compressible turbulence. The compressible dissipation has since been found to be less important than originally believed. In fact, the low turbulent Mach number asymptotics of [8] indicate it varies inversely with the Reynolds number and as a consequence is negligible in engineering flows, though not in low Reynolds number DNS. Compressible dissipation models are nonetheless included for completeness.

As the Taulbee and Van Osdol [5] compressible dissipation model requires additional transport equations, in the spirit of computational simplicity, that model will not be used. The closure proposed by Sarkar *et al.* [6] is based on ideas from linear acoustics and appears related to the initial value problem, [36]. It can be written as

$$\bar{\epsilon}_c = 3\alpha_s \bar{\epsilon}_s M_t^2 \tag{42}$$

with $\alpha_s = 1.0$ from DNS of decaying compressible turbulence; unfortunately this arrangement was deemed to lack universality [19]. Zeman [4] provides a model on the grounds that eddy shocklets occur in high speed flow and relating this assumption to the dilatational dissipation:

$$\bar{\epsilon}_c = 0.75(1 - \exp\{-[(\frac{3}{2}(1+\gamma)M_t - 0.1)/0.6]^2\})\epsilon_s \tag{43}$$

It has been shown by Blaisdell *et al.* [41] that Zeman's model gives incorrect scaling between ϵ_s and ϵ_c. Besides, the exponential dependence on M_t^2 delivers a steeper growth rate reduction compared to other models.

As has been mentioned in more recent DNS studies, [9, 14, 15, 42], have demonstrated that dilatational covariance closures with a M_t^2 scaling predict effects of compressibility when they are, in fact, very small. In an asymptotic analysis, Ristorcelli [8] has found that the compressible dissipation has an M_t^4 dependence and is inversely proportional to the turbulent Reynolds number:

$$\bar{\epsilon}_c = \left\{ \frac{16}{3\alpha_r^2} \left[I_2^s + 6I_1^s I_3^s \right] + \left(\frac{2}{5} \right)^5 \tau^2 \left[3\sigma^2 + 5\omega^2 \right] \cdot \right.$$
$$\left. \left[\frac{3}{5} I_3^r + \left(\frac{1}{15} \right)^2 \left[13\sigma^2 + 15\omega^2 \right] \tau^2 \alpha_r^2 I_1^r \right] \right\} \frac{M_t^4}{R_t} \bar{\epsilon}_s. \tag{44}$$

The parameters are $I_1^s = 0.3$, $I_2^s = 13.768$, $I_3^s = 2.623$, $I_1^r = 1.392$, $I_3^r = 3$ and $\alpha_r = 0.4 - 4$ is the Kolmogorov scaling coefficient. Also, M_t denotes the turbulent Mach number, that is $M_t^2 = \frac{2}{3}\langle k \rangle / c^2$ and R_t the turbulent Reynolds number $R_t = \bar{\rho} 4\langle k \rangle^2 / (9\epsilon_s \mu) Re$. The local speed of sound is given by $c^2 = T/M^2$. For high Reynolds number flows, in the absence of wall effects, viscous diffusion is negligible.

At this point the Reynolds stress equations have been closed and it is possible to compute the flow using a second-order closure. This is the subject of §5. However, there is a wide class of flows of engineering interest that can be treated using simple algebraic Reynolds stress models. An algebraic closure for the Reynolds stresses is therefore first developed.

4. A compressible algebraic Reynolds stress model. A quasi-explicit algebraic model for the Reynolds stresses is now derived. An algebraic Reynolds stress model comes from the fixed point solution of the evolution equations for the anisotropy tensor. These equations can be thought of as describing a

turbulence in a state of structural equilibrium: the fixed point solution corresponds to an exact solution of the Reynolds stress equations.

Several permutations of quasi-explicit algebraic Reynolds stress expressions exist:[20, 21, 22, 23, 24, 25, 26, 27, 28]. The qualifier "quasi-explicit" is used to indicate that, as the fixed point equations are nonlinear, the solution is given implicitly. A notable exception is the recent explicit algebraic model of Girimaji [28] who has found the exact *nonlinear* solution to the fixed point equations. The inception of our work predates [28] and our procedure follows precedents set by [20, 21, 26]. The polynomial representation methods will be used to obtain two-dimensional and three-dimensional versions of the algebraic turbulent stress models.

We use the *ansatz* introduced by Taulbee [21], to obtain the fixed point equation corresponding to the differential equation: the Lagrangian derivative in (17),

$$(45) \qquad \frac{D}{Dt}\left[\frac{a_{ij}}{\tau\sigma}\right] = 0,$$

is set to zero, which allows relaxation effects to be built into the Reynolds stress model. Equation (45) allows a relaxation of the anisotropy to its equilibrium value at the same rate that the relative strain relaxes to its equilibrium value, [21]. The combination of transport terms in (17) is set to zero following established algebraic stress modeling procedures:

$$(46) \qquad \frac{1}{\langle k \rangle}\left[\frac{\partial T_{ijk}}{\partial x_k} - \frac{\langle u_i'' u_j'' \rangle}{\langle k \rangle}\frac{\partial T_k}{\partial x_k}\right] - \frac{a_{ij}}{\langle k \rangle}\left[\frac{\partial T_k}{\partial x_k} - \tau\frac{\partial T_k^\epsilon}{\partial x_k}\right] = 0.$$

Applying these approximations results in a quasi-linear tensor expression for the anisotropy.

If $b_1 = \frac{8}{5} - \frac{2}{5}d_1$, $b_2 = \frac{1}{\bar{\rho}^2}\frac{2}{3}\tau_u\nu_0$, $b_3 = C_3 - 2d_2$, $b_4 = C_4 + 2d_2$, and

$$(47) \qquad g = \left[C_1\frac{\bar{\epsilon}}{\bar{\epsilon}_s} + C_{\epsilon 2} - 2 + (2 - C_{\epsilon 1})\frac{P}{\bar{\rho}\,\bar{\epsilon}_s} + \frac{\tau}{\sigma}\frac{D\sigma}{Dt} + \frac{2\tau}{3}(1 - 2d_2)S_{pp}(\langle u \rangle) + 2\frac{\mathcal{M} + \overline{p'd} - \bar{\rho}\,\bar{\epsilon}_c}{\bar{\rho}\,\bar{\epsilon}_s}\right]^{-1}$$

the algebraic fixed point form of the Reynolds stress anisotropy equation is written

$$(48) \qquad \mathbf{a} = -g\tau\left[b_1\mathbf{S}^\star + b_2\mathbf{R}^\star + b_3\left(\mathbf{a}\mathbf{S}^\star + \mathbf{S}^\star\mathbf{a} - \frac{2}{3}\{\mathbf{a}\mathbf{S}^\star\}\boldsymbol{\delta}\right) - b_4(\mathbf{a}\boldsymbol{\Omega} - \boldsymbol{\Omega}\mathbf{a})\right]$$

where the curly braces signify the trace. From this expression it is seen that the anisotropy tensor

$$(49) \qquad a_{ij} = a_{ij}(\mathbf{S}^\star, \boldsymbol{\Omega}, \mathbf{R}^\star)$$

is dependent on three second order tensors, two symmetric and one skew-symmetric.

4.1. A three-dimensional algebraic Reynolds stress model. Standard representation theory methods can be applied to obtain the solution $a_{ij} = a_{ij}(\mathbf{S}^\star, \boldsymbol{\Omega}, \mathbf{R}^\star)$ to (48). In contrast to the incompressible case the solution of (48) is now much more difficult inasmuch as the procedure now involves an additional tensor. Following standard methods the solution can be expressed as a finite 3-D tensor polynomial,

$$(50) \qquad \mathbf{a} = \sum_\lambda \mathcal{C}^\lambda T^\lambda$$

comprised of a linear combination of all the independent tensor products (generators) formed from the three primary tensors. The coefficients in the polynomial are functions of the independent invariants of the tensors.

For this problem the dimension of the [minimal] tensor base is $\lambda = 41$ (cf. Spencer [43]). This is very large and is unlikely to be used in practice.

The complexity presented by such a large tensor basis can be side stepped by simplifying approximation regarding the b_3 term. It has been argued [21, 27] that for the range of values used for the constant C_2 the inequality $C_3 \ll C_4$ holds and thus the term multiplied by C_3 will only have a small effect on the solution. This approximation decouples the contributions of $\mathbf{S}^\star$ and $\mathbf{R}^\star$ to $\mathbf{a}$. As the equation is linear the solution is determined using the superposition principle. This one allows to split the problem into two equations of lower tensor base dimension:

$$(51) \qquad \mathbf{a} = \mathbf{a}^S + \mathbf{a}^R$$

where $\mathbf{a}^S$ stands for the solution dependent on $\mathbf{S}^\star$,

$$(52) \qquad \mathbf{a}^S = -g\tau \left[b_1 \mathbf{S}^\star - b_4 (\mathbf{a}^S \mathbf{\Omega} - \mathbf{\Omega} \mathbf{a}^S) \right]$$

and $\mathbf{a}^R$ denoting the solution dependent on $\mathbf{R}^\star$

$$(53) \qquad \mathbf{a}^R = -g\tau \left[b_2 \mathbf{R}^\star - b_4 (\mathbf{a}^R \mathbf{\Omega} - \mathbf{\Omega} \mathbf{a}^R) \right].$$

The decomposition of $\mathbf{a}$ into portions dependent on $\mathbf{S}^\star$ and $\mathbf{R}^\star$ is unique.

Applying the results from [21] the strain dependent portion of the solution for the anisotropy tensor can be written

$$\mathbf{a}^S = -2C_\mu \tau \mathbf{S}^\star - 4\alpha_2 \tau^2 (\mathbf{S}^\star \mathbf{\Omega} - \mathbf{\Omega} \mathbf{S}^\star) - 8\alpha_3 \tau^3 (\mathbf{\Omega}^2 \mathbf{S}^\star + \mathbf{S}^\star \mathbf{\Omega}^2 - \frac{2}{3} \{ \mathbf{S}^\star \mathbf{\Omega}^2 \} \boldsymbol{\delta})$$

$$(54) \qquad -16\alpha_4 \tau^4 (\mathbf{\Omega} \mathbf{S}^\star \mathbf{\Omega}^2 - \mathbf{\Omega}^2 \mathbf{S}^\star \mathbf{\Omega}) - 32\alpha_5 \tau^5 \{ \mathbf{S}^\star \mathbf{\Omega}^2 \} (\mathbf{\Omega}^2 - \frac{1}{3} \{ \mathbf{\Omega}^2 \} \boldsymbol{\delta})$$

where $C_\mu = b_1 g (1 + \frac{7}{2} h_0^2 \omega^2) h_1$, $\alpha_2 = \frac{1}{2} b_1 b_4 g^2 h_2$, $\alpha_3 = \frac{3}{4} b_1 b_4^2 g^3 h_1$, $\alpha_4 = -\frac{3}{8} b_1 b_4^3 g^4 h_1$, $\alpha_5 = \frac{3}{8} b_1 b_4^4 g^5 h_1$, $h_0 = b_4 g \tau$, $h_1 = h_2 [1 + 2h_0^2 \omega^2]^{-1}$ and $h_2 = [2 + h_0^2 \omega^2]^{-1}$.

Using a similar procedure the portion of the Reynolds stress anisotropy dependent on the baroclinic dyad is written

$$\mathbf{a}^R = -2C_\mu \tau \mathbf{R}^\star - 4\alpha_2 \tau^2 (\mathbf{R}^\star \mathbf{\Omega} - \mathbf{\Omega} \mathbf{R}^\star) - 8\alpha_3 \tau^3 (\mathbf{\Omega}^2 \mathbf{R}^\star + \mathbf{R}^\star \mathbf{\Omega}^2 - \frac{2}{3} \{ \mathbf{R}^\star \mathbf{\Omega}^2 \} \boldsymbol{\delta})$$

$$(55) \qquad -16\alpha_4 \tau^4 (\mathbf{\Omega} \mathbf{R}^\star \mathbf{\Omega}^2 - \mathbf{\Omega}^2 \mathbf{R}^\star \mathbf{\Omega}) - 32\alpha_5 \tau^5 \{ \mathbf{R}^\star \mathbf{\Omega}^2 \} (\mathbf{\Omega}^2 - \frac{1}{3} \{ \mathbf{\Omega}^2 \} \boldsymbol{\delta})$$

in which the coefficients have the same form as those in $\mathbf{a}^S$ with the exception that b_1 is replaced by b_2. To obtain the full anisotropy tensor the two complex expressions (54) and (55) need to be added. In the light of the complexity of the three-dimensional formalism a two-dimensional formalism is developed.

4.2. A two-dimensional algebraic Reynolds stress model. A simpler and tractable two-dimensional treatment is possible. In many engineering flows the mean flow and the statistics of the turbulence are two-dimensional. The two-dimensional problem is less complicated as the number of tensor products necessary to express the solution is substantially reduced. The symbols $\mathbf{S}, \mathbf{\Omega}, \mathbf{R}$ now denote two-dimensional tensors.

It is necessary to recast the equation for the anisotropy in terms of the traceless 2-D tensors: $\underline{S}_{ij}^\star(\langle u \rangle) = S_{ij}(\langle u \rangle) - \frac{1}{2} S_{pp}(\langle u \rangle) \delta_{ij}^{(2)}$, $\underline{R}_{ij}^\star(\overline{\rho}, \overline{p}) = R_{ij}(\overline{\rho}, \overline{p}) - \frac{1}{2} R_{pp}(\overline{\rho}, \overline{p}) \delta_{ij}^{(2)}$. Here, the two-dimensional Kronecker symbol

15

is $\boldsymbol{\delta}^{(2)} \equiv [\delta_{ij}^{(2)}] = 1$ for $i = j = 1, 2$ and 0 otherwise. The pressure-strain model is then written:

$$\Pi_{ij}^\star - \overline{\rho}\,\epsilon_{ij}^\star = -C_1 \overline{\rho}\,\overline{\epsilon}a_{ij} + \overline{\rho}\langle k \rangle \left[\left[\frac{4}{5} + \frac{2}{5}d_1 \right] \underline{S}_{ij}^\star(\langle u \rangle) + \right.$$

$$[1 - C_3 + 2d_2] \left[a_{ip}\underline{S}_{pj}^\star(\langle u \rangle) + \underline{S}_{ip}^\star(\langle u \rangle)a_{pj} - \frac{2}{3}\underline{S}_{pq}^\star(\langle u \rangle)a_{pq}\delta_{ij} \right] -$$

$$[1 - C_4 - 2d_2][a_{ip}\underline{\Omega}_{pj}(\langle u \rangle) - \underline{\Omega}_{ip}(\langle u \rangle)a_{pj}] +$$

$$\frac{4}{3}d_2 S_{pp}(\langle u \rangle)a_{ij} - \left[\frac{4}{5} + \frac{2}{5}d_1 \right] S_{pp}(\langle u \rangle) \left[\frac{\delta_{ij}}{3} - \frac{\delta_{ij}^{(2)}}{2} \right] -$$

(56) $$2[1 - C_3 + 2d_2] \left[a_{ip}\left(\frac{\delta_{pj}}{3} - \frac{\delta_{pj}^{(2)}}{2} \right) - \frac{1}{3}a_{pq}\left(\frac{\delta_{pq}}{3} - \frac{\delta_{pq}^{(2)}}{2} \right)\delta_{ij} \right] S_{kk}(\langle u \rangle) \left. \right].$$

The pressure acceleration is written

(57) $$\mathcal{M}_{ij}^\star = -\frac{1}{\overline{\rho}}\frac{2}{3}\tau_u \nu_0 \langle k \rangle \underline{R}_{ij}^\star + \frac{1}{\overline{\rho}}\frac{2}{3}\tau_u \nu_0 \langle k \rangle R_{pp} \left[\frac{\delta_{ij}}{3} - \frac{\delta_{ij}^{(2)}}{2} \right].$$

The fact that both 2D and 3D expressions of the pressure-strain correlation model must give the same result when applied to two-dimensional mean flows will be used for our simplifications. Recasting the model in 2D is done to take advantage of the simplifications that result from the 2D structure.

Inserting the closures for the pressure-strain and mean acceleration terms, (56), (57) into the Reynolds stress equation, using the same *ansatz* regarding transport at a fixed point, the 2D analog of (48) is obtained:

$$\mathbf{a} = -g\tau \left[b_1 \mathbf{S}^\star + b_2 \mathbf{R}^\star + b_3 \left(\mathbf{a}\underline{S}^\star + \underline{S}^\star \mathbf{a} - \frac{2}{3}\{\mathbf{a}\underline{S}^\star\}\boldsymbol{\delta} \right) - b_4 \left(\mathbf{a}\underline{\Omega} - \underline{\Omega}\mathbf{a} \right) \right.$$

(58) $$\left. -b_5 \left(\frac{\boldsymbol{\delta}}{3} - \frac{\boldsymbol{\delta}^{(2)}}{2} \right) - b_6 \left(\mathbf{a}\left(\frac{\boldsymbol{\delta}}{3} - \frac{\boldsymbol{\delta}^{(2)}}{2} \right) - \frac{1}{3}\left\{ \mathbf{a}\left(\frac{\boldsymbol{\delta}}{3} - \frac{\boldsymbol{\delta}^{(2)}}{2} \right) \right\}\boldsymbol{\delta} \right) \right]$$

with $b_1 = \frac{8}{5} - \frac{2}{5}d_1$, $b_2 = \frac{1}{\overline{\rho}^2}\frac{2}{3}\tau_u \nu_0$, $b_3 = C_3 - 2d_2$, $b_4 = C_4 + 2d_2$, $b_5 = b_1 S_{pp}(\langle u \rangle) + b_2 R_{pp}(\overline{p}, \overline{p})$, $b_6 = 2b_3 S_{pp}(\langle u \rangle)$ and g having the same expression as in the 3-D algebraic equation. The two-dimensional polynomial solution of (58) is, as before, also written as

(59) $$\mathbf{a} = \sum_\lambda C^\lambda T^\lambda.$$

Unlike the three-dimensional solution, however, the generators now consist of only five tensor groups:

(60) $$\mathbf{T}^0 = \frac{\boldsymbol{\delta}}{3} - \frac{\boldsymbol{\delta}^{(2)}}{2}, \quad \mathbf{T}^1 = \underline{S}^\star, \quad \mathbf{T}^2 = \underline{S}^\star\underline{\Omega} - \underline{\Omega}\underline{S}^\star, \quad \mathbf{T}^3 = \underline{R}^\star, \quad \mathbf{T}^4 = \underline{R}^\star\underline{\Omega} - \underline{\Omega}\,\underline{R}^\star$$

for which there are five non-zero independent invariants,

(61) $$\sigma^2 = \{\underline{S}^{\star 2}\}, \quad \omega^2 = -\{\underline{\Omega}^2\}, \quad \{\underline{R}^{\star 2}\}, \quad \{\underline{R}^\star\underline{S}^\star\}, \quad \{\underline{S}^\star\underline{R}^\star\underline{\Omega}\}.$$

The fact that there are no other independent tensor generators [or invariants] can be verified using the 2×2 matrix identity:

$$2\mathbf{abc} = \mathbf{bc}\{\mathbf{a}\} + \mathbf{a}\{\mathbf{bc}\} + \mathbf{ac}\{\mathbf{b}\} - \mathbf{b}\{\mathbf{ac}\} + \mathbf{ab}\{\mathbf{c}\} + \mathbf{c}\{\mathbf{ab}\} -$$

(62) $$\mathbf{c}\{\mathbf{a}\}\{\mathbf{b}\} - \mathbf{a}\{\mathbf{b}\}\{\mathbf{c}\} + (\{\mathbf{ac}\}\{\mathbf{b}\} - \{\mathbf{acb}\})\boldsymbol{\delta}^{(2)}.$$

16

To obtain the solution to the algebraic equations for the anisotropy tensor, (58), a procedure similar to the one devised by [20] is used. Three 5×5 matrices $\mathcal{H}_\eta^\lambda$, $\mathcal{J}_\eta^\lambda$, $\mathcal{I}_\eta^\lambda$, are defined:

$$\mathbf{T}^\eta \underline{\mathbf{S}}^\star + \underline{\mathbf{S}}^\star \mathbf{T}^\eta - \frac{2}{3} \{ \mathbf{T}^\eta \underline{\mathbf{S}}^\star \} \boldsymbol{\delta} = \sum_\lambda \mathcal{H}_\eta^\lambda \mathbf{T}^\lambda$$

$$\mathbf{T}^\eta \underline{\boldsymbol{\Omega}}^\star - \underline{\boldsymbol{\Omega}}^\star \mathbf{T}^\eta = \sum_\lambda \mathcal{J}_\eta^\lambda \mathbf{T}^\lambda$$

(63)
$$\mathbf{T}^\eta \left(\frac{\boldsymbol{\delta}}{3} - \frac{\boldsymbol{\delta}^{(2)}}{2} \right) - \frac{2}{3} \left\{ \mathbf{T}^\eta \left(\frac{\boldsymbol{\delta}}{3} - \frac{\boldsymbol{\delta}^{(2)}}{2} \right) \right\} \boldsymbol{\delta} = \sum_\lambda \mathcal{I}_\eta^\lambda \mathbf{T}^\lambda$$

for which $\lambda = 0 - 4$. The elements of the matrices are determined from the above equations by making use of matrix relations stemming from the Cayley-Hamilton theorem. The 2-D tensor polynomial $\mathbf{a} = \sum_\lambda C^\lambda T^\lambda$ is introduced in both sides of relation (58). By making use of the above matrix identities the coefficients of the tensor polynomials are found to satisfy the following system of equations:

(64)
$$\mathcal{C}^\lambda = -g\tau \left[b_1 \delta_{1\lambda} + b_2 \delta_{3\lambda} + b_3 \sum_\eta C^\eta \mathcal{H}_\lambda^\eta - b_4 \sum_\eta C^\eta \mathcal{J}_\lambda^\eta - b_5 \delta_{0\lambda} - b_6 \sum_\eta C^\eta \mathcal{I}_\lambda^\eta \right].$$

The solution of this system of equations determines the model coefficients in the following algebraic expression for the anisotropy tensor

$$\mathbf{a} = -2C_\mu \tau \left[\mathcal{Q}_2 \underline{\mathbf{S}}^\star + (\mathcal{Q}_1 + \mathcal{Q}_3) b_3 g f_2 \tau \sigma^2 \left(\frac{2}{3} \boldsymbol{\delta} - \boldsymbol{\delta}^{(2)} \right) + \mathcal{Q}_2 b_4 g f_1 \tau (\underline{\mathbf{S}}^\star \underline{\boldsymbol{\Omega}} - \underline{\boldsymbol{\Omega}} \, \underline{\mathbf{S}}^\star) \right]$$

(65)
$$- 2C_\mu' \tau \left[\underline{\mathbf{R}}^\star + b_4 g f_1 \tau (\underline{\mathbf{R}}^\star \underline{\boldsymbol{\Omega}} - \underline{\boldsymbol{\Omega}} \, \underline{\mathbf{R}}^\star) \right]$$

suitable for two-dimensional mean flows. The eddy viscosities, C_μ and C_μ', are given by:

(66)
$$C_\mu = \frac{b_1 g f_1 / 2}{1 - \frac{2}{3} (b_3 g \tau)^2 \sigma^2 f_1 f_2 + 2(b_4 g f_1 \tau)^2 \omega^2}$$

(67)
$$C_\mu' = \frac{b_2 g f_1 / 2}{1 + 2(b_4 g f_1 \tau)^2 \omega^2}.$$

The $\mathcal{Q}_i$ coefficients are given by

(68)
$$\mathcal{Q}_1 = 1 + \frac{b_2}{b_1} \left[\frac{\{ \underline{\mathbf{S}}^\star \underline{\mathbf{R}}^\star \}}{\sigma^2} + 2 g f_1 \tau b_4 \frac{\{ \underline{\mathbf{S}}^\star \underline{\mathbf{R}}^\star \underline{\boldsymbol{\Omega}} \}}{\sigma^2} \right]$$

(69)
$$\mathcal{Q}_2 = 1 + \frac{2}{3} \frac{(b_3 g \tau)^2 \sigma^2 f_1 f_2}{1 + 2(b_4 g f_1 \tau)^2 \omega^2} (\mathcal{Q}_1 - 1) - \frac{b_3 b_5}{3 b_1} g f_2 \tau$$

(70)
$$\mathcal{Q}_3 = -\frac{b_5}{b_1 b_3} \frac{1 + 2(b_4 g f_1 \tau)^2 \omega^2}{2 g f_1 \tau \sigma^2}$$

(71)

with $f_1 = (1 + b_6 g \tau / 6)^{-1}$ and $f_2 = (1 - b_6 g \tau / 6)^{-1}$. Note that the direct effect of compressibility as reflected in the baroclinic dyad occurs in Q_1 and Q_2.

The high order of nonlinearity of the algebraic equations does not permit, in general, the construction of a fully explicit solution. Instead, an iterative approach is employed during the computations to generate the correct values. The algebraic solution is linearized by lagging the turbulence production term which contains the nonlinearity.

4.3. Discussion. To conclude this section some general statements regarding the behavior of the algebraic closure derived for the Reynolds stresses are highlighted. In §3 a closure for the Reynolds stress equations was obtained. In the present section the fixed point solution of the modeled second moment equations, under the condition of structural equilibrium, was obtained. For two-dimensional mean flows the compressible algebraic stress model can be symbolically written as

$$(72) \qquad \mathbf{a} = -\nu_{t0}\,\underline{\mathbf{S}}^\star - \nu_{t1}\,[\underline{\mathbf{S}}^\star\underline{\boldsymbol{\Omega}} - \underline{\boldsymbol{\Omega}}\,\underline{\mathbf{S}}^\star] - \nu_{t2}[\frac{2}{3}\boldsymbol{\delta} - \boldsymbol{\delta}^{(2)}] - \nu_{t0}^c\,\underline{\mathbf{R}}^\star - \nu_{t1}^c\,[\underline{\mathbf{R}}^\star\underline{\boldsymbol{\Omega}} - \underline{\boldsymbol{\Omega}}\,\underline{\mathbf{R}}^\star].$$

Note that products of the mean strain and the baroclinic dyad do not appear. This is due, for two-dimensional flows, to the relation $\mathbf{T}^\eta\underline{\mathbf{S}}^\star + \underline{\mathbf{S}}^\star\mathbf{T}^\eta - \frac{2}{3}\{\mathbf{T}^\eta\underline{\mathbf{S}}^\star\}\boldsymbol{\delta} = -2\{\mathbf{T}^\eta\underline{\mathbf{S}}^\star\}\mathbf{T}^0$; the generator comprised of the mean strain and baroclinic dyad product is redundant. Examining the above expression, the following observations can be made:

1. The first two terms are the same terms obtained in algebraic stress closure for two-dimensional [in the mean] incompressible flows.
2. The first two eddy coefficients are functions of the relative strain and the relative rotation as is the case in incompressible flows. They are now also functions of the turbulent Mach number and the gradient Mach number.
3. Neither of these eddy coefficients depend on baroclinic effects.
4. It is seen that in the absence of mean velocity gradients that the turbulence is anisotropic due to the mean baroclinic dyad. This anisotropy manifests itself in the deviatoric as well as diagonal terms.

It is useful to construct a simple example to see how the new effects influence the anisotropy. Consider a simple shear flow with a streamwise acceleration: let the Favré mean velocity, the mean density and the mean pressure gradients be represented by $U_{1,2}$, $U_{1,1}$, $\nabla\bar{\rho} = \bar{\rho}_{,2}$, and $\nabla P = P_{,1}$.

$$(73) \qquad a_{11} = -\frac{2}{3}\,\nu_{t0}\,U_{1,1} + \frac{1}{2}\,\nu_{t1}\,U_{1,2}^2 + \frac{1}{3}\,\nu_{t2} + \nu_{t1}^c\,U_{1,2}\,\bar{\rho}_{,2}\,P_{,1}$$

$$(74) \qquad a_{22} = \frac{1}{3}\,\nu_{t0}\,U_{1,1} - \frac{1}{2}\,\nu_{t1}\,U_{1,2}^2 + \frac{1}{3}\,\nu_{t2} - \nu_{t1}^c\,U_{1,2}\,\bar{\rho}_{,2}\,P_{,1}$$

$$(75) \qquad a_{33} = \frac{1}{3}\,\nu_{t0}\,U_{1,1} - \frac{2}{3}\,\nu_{t2}$$

$$(76) \qquad a_{12} = -\frac{1}{2}\,\nu_{t0}\,U_{1,2} - \frac{1}{2}\,\nu_{t1}\,U_{1,2}\,U_{1,1} - \nu_{t0}^c\,\bar{\rho}_{,2}\,P_{,1}$$

Several observations regarding the above algebraic expression for the anisotropy can be made:

1. The expression is the first [that we know of] rigorous indication of the direct role the baroclinic dyad plays in determining the Reynolds stresses.
2. The expression indicates that, for arbitrary mean deformation, the mean baroclinic dyad contributes to the deviatoric portions of the Reynolds stress.
3. The expression also indicates that the baroclinic dyad also changes the relative magnitude of the normal stresses. This effect only occurs for mean deformations that are rotational. For an irrotational mean deformation the baroclinic dyad makes no contributions to the normal stresses.
4. For a uniform mean velocity the baroclinic dyad is a source of anisotropy but only in the deviatoric portions of the anisotropy.
5. The expression indicates the inapplicability of any heuristic gradient transfer arguments for the Reynolds stresses in flows with important gradients of mean density and pressure.

While these results indicate the inapplicability of any form of eddy viscosity model for the stresses in compressible flows with arbitrary large density and pressure gradients some qualifications are in order. The presence of the baroclinic dyad is likely to be important only in rapidly accelerating aerodynamic flows or in combusting flows where one can expect the mass fluxes to be important. In the absence of these effects it appears that the parameterization of the Reynolds stresses in terms of powers of the mean deformation with modifications according to the compressibility of the fluctuations as those indicated in §3 is appropriate.

5. Computational investigations of free shear flows. The theory and results presented in the previous sections are now implemented over a very wide range of mean flow Mach numbers in the simulation of free shear flows. Simulations using second-order moment (SOM) closures as well as the quasi-explicit algebraic models are conducted. The numerical experiments are constructed with the intention of investigating several different issues of relevance to the prediction of compressible turbulent flows for engineering purposes.

In addition to assessing the sensitivity of the pressure-strain model to the different pressure-dilatation models we compare the computational results to what is expected from laboratory and numerical experiments. Of particular interest is the well known effect of compressibility on reduction of the spread rate of the mixing layer. The main objective is to assess the effectiveness of the compressibility corrections in reproducing the reduced growth rate of the free-shear layers with increasing Mach number - a phenomenon which is well documented experimentally [44]. We also study the adequacy of the algebraic stress closure with the results of the SOM simulations. In particular the Reynolds stresses and the anisotropy computed using both of these procedures are compared to solutions without the compressible corrections in order to assess the effects of the new pressure-strain closure on the anisotropy. Our intention is to further investigate the notion that the dramatic reduction of the mixing layer growth rate is due to the effects of compressibility on the pressure-strain and, consequently, its effect on the reduction of the turbulence shear stress.

5.1. Numerical method. The simulations are conducted using a finite difference scheme, following [45], second-order accurate in time and fourth-order accurate in space. The governing equations are integrated explicitly in time using the predictor-corrector finite difference scheme developed by Gottlieb and Turkel [46]. The Gottlieb-Turkel scheme is a higher order accurate variant of the MacCormack [47] predictor-corrector method. During a numerical sweep, the inviscid fluxes are alternatively differenced backward in the predictor step and forward in the corrector step. Fourth-order central differences are used for the viscous and heat flux terms as well as for the derivatives in the source vector. To maintain stability, it is required that the CFL number be less than $2/3$. To prevent numerical oscillations in regions of large gradients a smoothing scheme devised by MacCormack and Baldwin [48] is employed. The method, as outlined in [45], adds artificial viscosity that is very small everywhere except in the regions where the pressure oscillates.

All simulations are conducted on a uniformly spaced grid in the computational domain. By means of a coordinate transformation the mesh is transversally compressed in the physical domain in the region corresponding to the mixing layer.

The physical domain is a rectangular box defined by the set of points (x, y), in which x represents the streamwise coordinate and y the transversal coordinate. The grid overlaying the computational domain of size $x\delta_\omega \times y\delta_\omega$ has 100×60 points, where the vorticity thickness $\delta_\omega = (u_1 - u_2)/(\partial\langle u\rangle/\partial y)_{max}$, the brackets $\langle\rangle$ denoting the averaged value. In this nondimensionalization, the reference length scale is the magnitude

of the vorticity thickness at the inlet. The initial profile for the mean axial velocity is adjusted such that the resulting nondimensional vorticity thickness at the inlet is equal to one. The values of the physical dimensions are $(x, y) = [80, 20]$ for the mixing layer. To evaluate the grid sensitivity the number of grid points is increased by a factor of 1.5. The change in the steady-state values of the peak of the turbulent stresses is less than 2 percent.

To accelerate convergence to the stationary state, a local time stepping technique is used. The convergence criterion is imposed so that the global averaged residual profile attained is stationary for each dependent variable. Although more stringent criteria can be sought, it is known, [49], that predictor-corrector schemes are limited in their ability to achieve very high rates of residual reduction.

Due to the nonlinearity of the destruction terms, the $k - \epsilon$ equations display a stiffness which can either generate numerical instabilities or increase the computational time. In order to avoid these inconveniences the turbulence source terms are treated implicitly. The $k - \epsilon$ destruction terms are decoupled by suitable manipulation of the ϵ/k ratio, considered as a known quantity from the previous time step.

Initial and boundary conditions. The initial fields are obtained by propagating the inflow conditions throughout the entire domain; hence, the flow has to sweep the domain at least one time to obtain meaningful results. For ease of computation, the inflow initial conditions (IC) for the flow variables are assumed to be a smoothed step (hyperbolic tangents for the axial velocity or species) or a smoothed hat profile (for turbulence quantities). Uniform profiles are assigned at the inlet to the static pressure, to the static temperature and, by virtue of the equation of state, to the static density.

The boundary conditions (BC) are set according to the elliptic nature of the problem on all four boundaries. The inflow BC are fixed (Dirichlet) for all primary variables in the supersonic and subsonic regions with one exception. For the portions where the flow is subsonic the pressure is allowed to adjust to the characteristic waves through a Neumann boundary condition. At the outflow and outer boundaries zero gradient (Neumann) conditions are applied due to their non-reflective properties in relation with the outgoing waves. In the mixing layer, the static pressure, temperature and density in the two free stream layers are matched. This isolates the contributions to the layer growth to those due solely to the variation of the reference Mach number.

Free-shear flow parameters. The magnitude of the effects of compressibility are often parameterized by the convective Mach number [50]. In our formulation the expression for the convective Mach number is $M_c = M(1 - r_v)/2$, where $r_v = u_2/u_1$ is the axial velocity (u) ratio. A wide range of values of M_c including both subsonic and supersonic regimes are considered: $0.2 < M_c < 2.0$. The convective Mach number is varied by keeping the velocity ratio constant and varying the reference Mach number M. The reference Reynolds number is $Re = 5 \times 10^6$, while all the other nondimensional parameters are kept constant as well. The subscript 1 refers to the high-speed stream value, while the subscript 2 refers to the low-speed stream value in the mixing layer. No jet simulations are shown in this article; they can be found in [37].

In the results presented, the spatial coordinate, for the hydrodynamic variables, are given by η. In the mixing layer, $\eta = \frac{y - y(\hat{u}=0.5)}{x}$, where $\hat{u} = \frac{\langle u \rangle - u_2}{u_1 - u_2}$. Unless otherwise specified, the results shown are from computations [ARSM and SOM] with models based on the dilatational models of [8].

After an initial period of flow development a linear growth rate of the shear layers is attained. In the fully

developed regime, when a linear growth rate has been established, the mean velocity and the normalized Reynolds stresses display self-similar behavior. The spread rate of a turbulent shear layer, in the self-similar region, is conventionally expressed as $d\delta_u/dx = C_\delta(1 - r_v)/(1 + r_v)$ where δ_u could be either the 10 percent visual thickness of the shear layer based on the normalized velocity profile or the vorticity thickness, and C_δ is a constant (approximately). As the present article is concerned with compressible corrections to the turbulence moment equations no plots of the mean flow quantities are given; the mean field variables are quite typical and can be seen in the literature, [11, 51, 52].

5.2. Mixing layer simulations. The primary concerns of this article are with 1) a representation of the effects of compressibility as they appear in the pressure-strain covariance and 2) the construction of an algebraic Reynolds stress model useful for engineering calculations. Studies related to both these issues, for the $M_c = 1.07$ mixing layer configuration, are shown in the first two figures. The Reynolds stresses and the production/dissipation ratio obtained for ARSM and SOM calculations are shown in Figures 1 and 2. Also shown, as a double check, are curves based on an *a priori* evaluation of the algebraic stress model; the data from a SOM calculation is used as input to the ARSM. The neglect of turbulent transport in the algebraic stress model is reflected in differences in the normal stresses at the centerline. In general the *a priori* evaluated ARSM curves follow closely the computed ARSM values indicating that for this flow the neglect of transport in the moment transport equations is justified. The algebraic approximation is, as has been verified at several different convective Mach numbers, suitable for an investigation of trends in this flow configuration.

Also shown in Figures 1 and 2 is the SOM computation without compressibility corrections [NC - no compressibility]. The effect of the compressibility corrections manifest themselves as decreases in the centerline values of $\langle uu \rangle, \langle uv \rangle$ and $\langle vv \rangle$ of approximately $16\%, 25\%$ and 24% respectively. This is consistent with that seen in DNS. In addition, the streamwise normal stress suffers a smaller reduction than the other Reynolds stresses. This, as will be seen, will manifest itself in an increase in the streamwise normal anisotropy.

The production/dissipation ratio is shown in the bottom of Figure 2. The average level of P/ϵ for the compressible case is smaller than the incompressible case; this is consistent with the reduced turbulent kinetic energy of the compressible flow. While the overall level of the production is smaller it is interesting to note that at one location in the mixing layer, the centerline, P/ϵ is nominally higher. It has been conjectured that this might be due to the higher relative strain rates compressible flows may be able to sustain. This is an issue that further DNS may resolve.

Figure 3 displays the vorticity thickness. Vorticity thickness spread rates as predicted by the SOM simulations, with and without (NC) the compressibility correction, are shown on the top of Figure 3. It is seen, that even with such modest contributions from compressibility, scaling as they do with M_t^2, a sizable change in growth rate is seen. The variation of M_t with M_c is shown in Figure 5.

Figure 3 also displays the different components of the pressure-strain tensor computed from the SOM simulation with and without (NC) the compressibility correction. The different components of the pressure-strain are all reduced by about the same amount. This is precisely the behavior seen, in both direction and magnitude, in the recent DNS [15] – see Figure 4.18.

Reynolds stress anisotropy. In Figure 4 the computed values of the centerline Reynolds stress anisotropies are shown. At low values of compressibility the anisotropy has values similar to that of simple incompressible

shears. At higher levels the anisotropy behaves very much like the compressible shear DNS; more of the energy of the turbulence is in the streamwise component as made clear by the increase in a_{11}. This is at the expense of the crosstream component, $\langle vv \rangle$, which is reduced. This is, as shall be discussed further, due to the reduction of intercomponent energy transfer due to the compressible aspect of the pressure-strain. There is also a reduction in the shear stress as is seen in compressible DNS.

Comparisons with laboratory Reynolds stresses. The effects of the new compressible models on the anisotropy is shown in Figure 4. Unfortunately, in the laboratory situation, the spanwise Reynolds stresses are rarely measured. As a consequence the anisotropy is not known and one returns to primitive variables.

The maximum values of diverse Reynolds stresses in the mixing layer are plotted as function of the convective Mach number in Figure 4. In this figure σ_u and σ_v represent, respectively, the $\langle uu \rangle$ and $\langle vv \rangle$ Reynolds stresses nondimensionalized by the square of the velocity difference across the layer. Also shown are the experimental results of Elliot and Samimy [53]. Underlying this comparison is, of course, the implicit assumption of self-similarity. The maximum Reynolds stresses decrease with compressibility. In the present simulations, however, the peak values of the turbulence intensities (axial and transverse) do not vary as strongly as in the laboratory findings of Goebel and Dutton [54]. In fact the present simulations are closer to the results of either [54] or [53] than either [54] or [53] are to each other.

There appears to be a discrepancy. A survey of the diverse compressible DNS indicates that a_{11} increases with compressibility. This implies that $\langle uu \rangle$ decreases faster than $\langle vv \rangle$. [Figure 9 of [14] is the most comprehensive presentation of this trend.] This does not appear to be the case in the laboratory experiments. In the mixing layer of [53] $\langle uu \rangle$ decreases more rapidly than $\langle vv \rangle$ for all M_c implying that a_{11} decreases with increasing compressibility contrary to DNS results. In [54] $\langle uu \rangle$ decreases more rapidly than $\langle vv \rangle$ for low M_c; while at moderate M_c, $\langle uu \rangle$ decrease less rapidly than $\langle vv \rangle$ in accord with DNS results. No explanation for this discrepancy between laboratory and numerical data is known.

The pressure-strain tensor. The effects of compressibility on the Reynolds stresses are believed to be the source of the dramatic influence on the spread rate as the convective Mach number increases. The physical mechanisms responsible for these phenomena were once believed to be the compressible dissipation and pressure-dilatation which caused a decrease in the Reynolds stresses due to an overall decrease in k. This was accompanied by no substantial changes in the anisotropy. As discussed in §1, recent simulations suggest that compressibility causes a turbulent shear stress reduction due to a reduction in its associated anisotropy. This is a statement that compressibility manifests itself structurally, not energetically. The reduction in the anisotropy leads, of course, to a reduction in k and ultimately in the mixing layer growth rate.

More recent simulations, [9, 14, 15, 16] all seem to indicate that the major changes in the shear stress are due to the effect of compressibility on the pressure-strain covariance. Figure 6 is an illustration of this idea: Figure 6 depicts the different components of pressure-strain tensor and its trace [the pressure dilatation] at the centerline of the mixing layer. Figure 6 is patterned after Vreman *et al.'s* [14] Figures 3 and 9. The behavior of all the components of the pressure-strain, shown in Figure 6, are very much in accord with the figures of [14]. The only notable difference is the relative levels of Π_{22} and Π_{33}. The trends are very much the same and the relative behavior – a commensurate across the board reduction with M_c – is very much in accord with [15].

The behavior of the pressure-strain illustrated in Figure 6 is very much in keeping with the current under-standing of the mechanism for the reduction of the turbulence energy by the reduction of the shear stress: the only source for the kinetic energy is in the $\langle uu \rangle$ component and its production is proportional to $\langle uv \rangle$. The reduction [in magnitude] of Π_{11} and Π_{22} means that less energy generated in the $\langle uu \rangle$ equation is transferred to $\langle vv \rangle$ [by Π_{22}]. As $\langle vv \rangle$ has no production $\langle vv \rangle$ is much smaller. As consequence of the fact that the production of $\langle uv \rangle$ is proportional $\langle vv \rangle$ much less $\langle uv \rangle$ is produced and much less $\langle uu \rangle$ is produced. This can be seen by the considering the truncated forms of the second-order moment equations:

$$(77) \qquad \frac{D}{Dt}\langle uu \rangle \sim -\langle uv \rangle U_{1,2} + \Pi_{11} + ...$$

$$(78) \qquad \frac{D}{Dt}\langle vv \rangle \sim \ \ \Pi_{22} + ...$$

$$(79) \qquad \frac{D}{Dt}\langle uv \rangle \sim -\langle vv \rangle U_{1,2} + \Pi_{12} + ... \ \ .$$

The thesis of [15] provides a schematic of the above process. The behavior of the Reynolds stresses and the pressure-strain indicated by Figures 2 and 6 is consistent with the mechanism for the reduction just delineated. Specifically, the fact that less of the $\langle uu \rangle$ energy is transferred to the other components of the Reynolds stress means that the anisotropy, $a_{11} = 2b_{11}$, must increase as seen in all the DNS. Note also that the pressure-dilatation as derived by the asymptotic procedure in [8] is extremely small; negligible in comparison to the pressure-strain. Yet its use to obtain the deviatoric portions of the pressure-strain produces a very sizable reduction in the shear stress and the growth rate.

Gradient Mach number. Sarkar [16] and earlier work cited therein have drawn attention to the gradient Mach number as a potentially useful parameterization of the effects of compressibility. Many of the effects of compressibility, as indicated by diverse DNS, have been observed to become more apparent as the gradient Mach number increases. Shown in the bottom of Figure 5 is the gradient Mach number using the definition $M_g = \frac{2}{3} M_t \sigma \langle k \rangle / \epsilon_s$. The definition of the gradient Mach reflects the fact that the Kolmogorov scaling, $\epsilon \sim \langle k \rangle^{3/2} / \ell$ has been used to eliminate the length scale in the definition $M_g = \sigma \ell / c$. In DNS, the length scale ℓ is determined from the two-point correlation; no such opportunity occurs in single-point closures. Both the DNS, for example Figure 4.29 in [15], and the SOM simulation indicate a similar decrease in rate of increase of M_g with M_c. The decrease seems to occur at lower M_c in the DNS. This is likely to be related to the different length scales used.

One of the noteworthy observations made of the effects of compressibility is their tendency to saturate, [11]. In the bottom of Figure 5 the rate of increase of the maximum turbulent Mach decreases at higher convective Mach numbers. This is line with observations of [11].

Kolmogorov scaling. While in DNS a length can be determined from the two-point correlation, no such possibility exists for single-point closures. Yet a length scale, reflecting the two-point nature of the turbulence problem, is required. The length scale appearing in the Kolmogorov inertial range scaling, $\epsilon \sim \langle k \rangle^{3/2} / \ell$, was used in [8].

There is a proportionality coefficient, α, in the Kolmogorov scaling $\alpha = \overline{\epsilon}_s \ell / (2\overline{k}/3)^{3/2}$. For infinite Reynolds number isotropic turbulence $\alpha \sim 1$. For finite but large Reynolds number anisotropic turbulence undergoing deformation the Kolmogorov scaling is likely to be useful but α is likely to be a flow dependent quantity. Sreenivasan [55] has made some studies of the variation of the Kolmogorov scaling coefficient: [55] has found

values of α ranging between $0.4 - 2$ for diverse incompressible simple shear flows. To allow for the expected variability of α two different values of are used in many of the simulations. The value of α does not change any of the trends and does not seem to have too strong an effect on the energy at the centerline as seen in Figures 4 and 5. It does however effect the mixing layer spread rate as can be seen in Figure 8.

Mixing layer growth rates. Settles and Dodson [44] have compiled a very large number of experimental results. These are shown in Figures 7 and 8. The experimental curves come from the experiments of [50, 54, 56, 57, 58, 59, 60, 61]. The scatter in the data reflects the fact that different experiments are done in different wind tunnels, with different inlet configurations and with different reservoirs. The computational curves shown in Figures 7 and 8 reflect two different but complementary investigations. As the "Langley curve" [62] has been a popular benchmark it has also been included. The well known reduction in the mixing rate with increasing M_c is seen in all the data.

Figure 7 reflects computations using the "energetic" approaches. A $k - \epsilon$ scheme has been used to calculate the mixing layer growth and the only compressible corrections are in the k equation; the Reynolds stresses are closed with the usual incompressible eddy viscosity [Boussinesq] approximation. The compressible dissipation and pressure-dilatation models of Zeman [4], Sarkar *et al.* [6, 38], Ristorcelli [8] are used in the $k - \epsilon$ scheme. Figure 7 indicates that the results based on the models of Zeman [4], and Sarkar *et al.* [6, 38] capture the mixing layer reduction. The reduction of the mixing layer growth rate has been captured by similar mechanisms in both models; most of the suppression is provided by a substantial amount of additional dissipation that comes from the compressible dissipation models. As was pointed out in §1, the compressible dissipation, as has been indicated by DNS and by asymptotic analysis, is not important in these flows. Any arbitrarily dissipative term added to the k equation, appropriately calibrated and scaled, would produce such agreement for the mixing layer growth. Moreover, as with all energetic approaches, there is no possibility of accounting for the very important structural changes that appear in the anisotropy.

As indicated by Figure 7 the pressure-dilatation model of [8], with $\alpha = 2$, accounts for a nominal suppression of the growth rate. The compressible dissipation being negligible in analysis of [8] is not included in this calculation. From incompressible DNS, [63] it can be argued that a value of $\alpha \approx 1$ might be more appropriate. As the pressure dilatation scales with α^2 a value of $\alpha \approx 1$ would decrease the pressure-dilatation effects by a factor of four.

Figure 8 reflects a computation using the compressible algebraic Reynolds stress model. This is exactly the same computation as given in the Figure 7 with the exception that the algebraic Reynolds stress approximation now includes the effects of compressibility in the pressure-strain covariance representation used to close the second-moment equations. Note the substantial changes on the layer growth rate prediction that include the effects of compressibility on the Reynolds stresses produces. The change is more drastic for the Ristorcelli modeling than the Sarkar modeling; this is to be expected as the majority of the growth rate reduction using the earlier Sarkar modeling was built into a dissipative term and the relative change is small.

The algebraic model built upon dilatational closures of [8] shows improvement over the results from a simple $k - \epsilon$ scheme. Figure 8 depicts the outcomes of the computations with the Ristorcelli [8] based algebraic closures for two values of the Kolmogorov scaling coefficient. The results for $\alpha = 0.4$ with both the pressure-strain and pressure-dilatation provide a modest decrease in the spread rate; handily matching that predicted with simply the pressure-dilatation with $\alpha = 2$. The ARSM calculation is substantially changed when $\alpha = 2$;

if α were an undefined constant one might be tempted to set it so as to match the reduction in spread rate indicated by the data. Given that little is known about α [though it is sure to be in the range 0.4-2.0 and most likely $\alpha \approx 1$] these issues must be left to future DNS work.

It is concluded that the present pressure-strain modeling method based on the extension of the well-established incompressible procedure, in which the trace-free constraint is relaxed, does rationally account for a significant portion of the reduction in shear stress and growth rate. This procedure is considered a leading order contribution to the compressible turbulence shear stress problem. The possibility that additional compressible corrections to the pressure-strain, addressing physics not able to be accounted for using this constitutive relation methodology, may require consideration.

6. Some issues in compressible turbulence modeling. In our effort to obtain a closure for the effects of compressibility a few issues, already alluded to, have become clearer. These issues are now highlighted.

The baroclinic dyad. The procedure invoked to obtain the algebraic Reynolds model indicates that the baroclinic dyad is a source of turbulence. This, of course, can be anticipated by inspection of the second-order moment equations. The consequence is that an eddy viscosity representation for the Reynolds stresses is, from first principles, inappropriate for classes of flows in which the mass fluxes are important.

The presence of the baroclinic dyad is likely to be important only in rapidly accelerating aerodynamic flows such as through shocks or in hypersonic situations. The baroclinic dyad is also likely to be important in combusting flows where one can expect the mass fluxes to be important. In noncombusting supersonic flows it appears that a parameterization of the Reynolds stresses in terms of the mean deformation with modifications according to the compressibility of the fluctuations as those derived in §3.1 appears appropriate.

A length scale for single-point models of compressible turbulence. Much of the work described here is based on the leading order asymptotic analysis of [8]. In [8] the effects of the non-zero divergence of compressible turbulence was parameterized by several two-point integrals made nondimensional by a length scale. For single-point turbulence closures the length scale is typically determined by the Kolmogorov inertial range scaling, $\epsilon \sim k^{3/2}/\ell$.

For compressible turbulence of interest to supersonic aerodynamic flows the cascade mechanism will be comprised of the usual nonlinear solenoidal modal interactions. The Kolmogorov scaling is expected to be valid in the weakly compressible limit. However, given the notable behavior seen in simulations with increasing compressibility of a length scale, see Figure 4.28 of the recent [15], one might expect the coefficient of proportionality, what we have called α, to be a function of compressibility. That this might be the case is also suggested by different instability modes that appear in the compressible flows. Studies similar to the incompressible studies shown in [63] appear to be both interesting and very relevant to issues of compressible turbulence modeling.

Experimental differences in numerical and laboratory data. There appears to be a unanimous agreement in the DNS that, with increasing gradient or convective Mach number, a_{11} increases while a_{22} and a_{12} both decrease. This trend does not appear in the laboratory mixing layer experiments. At low M_c, $\langle uu \rangle$ appears to decrease more rapidly, with increasing compressibility, than $\langle vv \rangle$. This implies that a_{11} decreases with

compressibility in contradistinction to DNS results. It is crucial to understand the cause for the differences between the DNS and the laboratory flows of the $\langle uu \rangle$ Reynolds stress behavior; turbulence models are based on intuition gleaned from DNS data but are used to predict engineering flows that are more similar to laboratory flows. The present computational results are closer to either of the laboratory experiments of [53] or [54] than the laboratory experiments of [53] or [54] are to each other. Earnest speculation on the source of the differences in the two experiments and facilities is required.

7. Summary and conclusions. Progress towards the development of a compressible turbulence closure, starting at the level of second-order moment equations, has been described. Modeling from the second-order level accommodates important structural changes that appear in the anisotropy and are a feature and a function of compressibility. In the second-order moment equations the compressible contributions to the pressure-strain covariance have been obtained. The pressure-strain has been closed by assuming that, as is consistent with the weakly compressible limit, it can be modeled as a tensor polynomial linear in the Reynolds stresses. The difference from the incompressible case is that the trace of the compressible strain is not zero; it is set equal to the pressure-dilatation for which models exist. The compressible pressure-strain closure features a dependence on several turbulence descriptors: the turbulent Mach number, the relative strain, the gradient Mach number, the production and the dissipation. As a consequence the coefficients in the compressible pressure-strain closure are not constants but functions of the compressible parameters.

In addition to devising a closure for the pressure-strain, a closure for the mean acceleration/mass flux terms appearing in the Reynolds stress equations has also been developed. For the flows studied in this article, which are limited to the flows for which relevant experimental data are available, the acceleration/mass flux moments are not important. The mass flux terms will be important in the combusting or hypersonic flows which motivated the thesis [37], of which this article treats one aspect.

Having closed the compressible Reynolds stress equations standard tensor representation procedures have been used to produce a compressible algebraic Reynolds stress model useful for flows near a structural equilibrium. A noteworthy item of this portion of the work is that the role that the mean pressure and mean density gradients plays on the Reynolds stresses is immediately seen. As a consequence, it is seen that the baroclinic dyad can, in the absence of mean velocity gradients, contribute to the anisotropy of the turbulence. It is also seen that the mean bulk dilatation contributes to the anisotropy in a way that is quite different from an irrotational strain.

The mathematical results developed here have been implemented in mixing layer computations spanning a wide range of mean flow Mach numbers. In this article the discussion has been limited to the compressible mixing layer for which a sizable amount of literature exists. The calculations presented have been organized along two themes: 1) an investigation of the effects of compressibility as related to the compressible pressure-strain and the Reynolds stresses and 2) a validation of the algebraic Reynolds stress model predictions.

The computations with the compressible pressure-strain indicate that the present modeling [which does not have undefined tunable constants] produces precisely the behavior seen in the DNS of [14] and [15]; there is a commensurate reduction, with increasing convective Mach number, of all the components of the compressible pressure-strain tensor. The changes in the pressure-strain lead, as is established by DNS of several different flows [14, 15, 16], to changes in the anisotropy of the Reynolds stresses. The changes predicted by the modeling for the normal and shear anisotropies are very consistent, in trend, with DNS data and especially

with the DNS of the mixing layer of [14] — the flow configuration most similar to the one treated in this article. Comparisons between the computational predictions and laboratory resutls for the Reynolds stress and their behavior with increasing compressibility is poor. This is due to unknown experimental issues: the agreement between even the different laboratory experiments is poorer than the agreement between the numerical and experimental results.

All the laboratory data do however agree on the trend of the mixing layer growth rate with increasing compressibility: it decreases. The computational experiments conducted indicate that sizable reductions in the mixing layer growth rate accompany changes in the anisotropy of the turbulence due to the compressible aspects of the pressure-strain covariance.

REFERENCES

[1] S. K. LELE (1994), *Compressibility effects on turbulence.* Ann. Rev. Fluid Mech., 26, p. 211.

[2] E. J. GUTMARK, K. C. SCHADOW, K. H. YU (1995), *Mixing enhancement in supersonic free shear flows.* Ann. Rev. Fluid Mech., 27, p. 375.

[3] E. F. SPINA, A. J. SMITS, S. K. ROBINSON (1994), *The physics of supersonic boundary layers.* Ann. Rev. Fluid Mech., 26, p. 287.

[4] O. ZEMAN (1990), *Dilatation dissipation: the concept and application in modelling compressible mixing layers.* Phys. Fluids A, 2(2), p. 178.

[5] D. B. TAULBEE, J. VANOSDOL (1991), *Modeling turbulent compressible flows: the mass fluctuating velocity and squared density.* AIAA Paper 91-0524.

[6] S. SARKAR, G. ERLEBACHER, M. Y. HUSSAIN, H. O. KREISS (1991), *The analysis and modelling of dilatational terms in compressible turbulence.* J. Fluid Mech., 227, p. 473.

[7] P. A. DURBIN, O. ZEMAN (1992), *Rapid distortion theory for homogeneous compressed turbulence with application to modeling.* J. Fluid Mech., 242, p. 349.

[8] J. R. RISTORCELLI (1997), *A pseudo-sound constitutive relationship for the dilatational covariances in compressible turbulence: An analytical theory.* J. Fluid Mech., 347, p. 37. Also available as ICASE Report 95–22.

[9] A. SIMONE, G. N. COLEMAN, C. CAMBON (1997), *The effect of compressibility on turbulent shear flow - a rapid-distortion-theory and direct-numerical-simulation study.* J. Fluid Mech., 330, p. 307.

[10] J. R. VIEGAS, M. W. RUBESIN (1991), *A comparative study of several compressibity corrections to turbulence models applied to high-speed shear layers.* AIAA Paper 91-1783.

[11] S. SARKAR, B. LAKSHMANAN (1991), *Application of a Reynolds stress turbulence model to the com-*

pressible shear layer. AIAA J., 29(5), p. 743.

[12] C. G. SPEZIALE, S. SARKAR (1991), *Second order closure models for supersonic turbulent flows.* ICASE Report 91–9, NASA Langley Research Center, Hampton, VA. Also available as NASA CR 187508.

[13] R. ABID (1994), *On the prediction of equilibrium states in homogeneous compressible turbulence.* NASA CR 4570, NASA Langley Research Center, Hampton, VA.

[14] A. W. VREMAN, N. D. SANDHAM, K. H. LUO (1996), *Compressible mixing layer growth rate and turbulence characteristics.* J. Fluid Mech., 320, p. 235.

[15] J. B. FREUND, P. P. MOIN, S. K. LELE (1997), *Compressibility effects in a turbulent annular mixing layer.* Department of Mechanical Engineering Report TF-72, Stanford University, Stanford, CA.

[16] S. SARKAR (1995), *The stabilizing effect of compressibility in turbulent shear flow.* J. Fluid Mech., 282, p. 163.

[17] G. A. BLAISDELL, S. S. SARKAR (1993), *Investigation of the pressure-strain correlation in compressible homogeneous turbulent shear flow.* In *Transitional and Turbulent Compressible Flows*, Proceedings of the 1993 ASME Fluids Engineering Conference, Washington, DC, June 21–24, 1993, FED-Vol. 151, pp. 133–138.

[18] C. G. SPEZIALE, R. ABID, N. M. MANSOUR (1995), *Evaluation of Reynolds stress turbulence closures in compressible homogeneous shear flows.* Z. Angew. Math. Phys., S717.

[19] A. M. EL BAZ, B. E. LAUNDER (1993), *Second-moment modelling of compressible mixing layers.* In W. Rodi, F. Martelli, editors, *Engineering Turbulence Modelling and Experiments*, v. 2, pp. 63–72. Elsevier Publishing Co., North Holland.

[20] S. B. POPE (1975), *A more general effective-viscosity hypothesis.* J. Fluid Mech., 72, p. 331.

[21] D. B. TAULBEE (1992), *An improved algebraic Reynolds stress model and corresponding nonlinear stress model.* Phys. Fluids A, 4(11), p. 2555.

[22] W. RODI (1976), *A new algebraic relation for calculating the Reynolds stresses.* ZAMM, 56, p. 219.

[23] B. E. LAUNDER (1975), *On the effects of a gravitational field on the turbulent transport of heat and momentum.* J. Fluid Mech., 67, p. 569.

[24] W. RODI (1980), *Turbulence models for environmental problems.* In W. Kollmann, editor, *Prediction Methods for Turbulent Flows*, pp. 260–349. Hemisphere Publishing Co., New York, NY.

[25] C. G. SPEZIALE (1991), *Analytical methods for the development of Reynolds-stress closures in turbulence.* Ann. Rev. Fluid Mech., 23, p. 107.

[26] T. B. GATSKI, C. G. SPEZIALE (1993), *On explicit algebraic stress models for complex turbulent flows.* J. Fluid Mech., 254, p. 59.

[27] D. B. TAULBEE, J. R. SONNENMEIER, K. M. WALL (1994), *Stress relation for three-dimensional turbulent flows.* Phys. Fluids A, 6(3), p. 1399.

[28] S. S. GIRIMAJI (1996), *Fully-explicit and self-consistent algebraic Reynolds stress model.* Theoret. Comput. Fluid Dynamics, 8, p. 387.

[29] A. FAVRE (1969), *Statistical equations of turbulent gases.* In *Problems of Hydrodynamics and Continuum Mechanics*, pp. 37–44, SIAM, Philadelphia.

[30] B. E. LAUNDER, G. J. REECE, W. RODI (1975), *Progress in the development of a Reynolds-stress turbulence closure.* J. Fluid Mech., 68, p. 537.

[31] C. G. SPEZIALE, S. SARKAR, T. B. GATSKI (1990), *Modeling the pressure-strain correlation of turbulence - an invariant dynamical systems approach.* J. Fluid Mech., 227, p. 245.

[32] J. R. RISTORCELLI, J. L. LUMLEY, R. ABID (1995), *A rapid-pressure covariance representation con-*

sistent with the Taylor-Proudman theorem materially-frame-indifferent in the 2D limit. J. Fluid Mech., 292, p. 111.

[33] J. L. LUMLEY (1970), *Towards a turbulence constitutive relationship.* J. Fluid Mech., 41, p. 413.

[34] J. L. LUMLEY (1978), *Computational modeling of turbulent flows.* Adv. Appl. Mech., 18, p. 123.

[35] J. R. RISTORCELLI (1997), *Towards a turbulence constitutive relation for geophysical flows.* Theoret. Comput. Fluid Dynamics, 9, p. 207. ICASE Report 96-66. Part of the Proceedings of "New Directions in Geophysical Fluid Dynamics and Turbulence".

[36] J. R. RISTORCELLI (1998), *Some results relevant to the statistical closures for compressible turbulence.* ICASE Report 98–1, NASA Langley Research Center, Hampton, VA. Part of the Proceedings of ICASE/LaRC/AFOSR Symposium on Modeling Complex Turbulent Flows, Aug. 11-13, Kluwer Publications.

[37] V. ADUMITROAIE (1997), *Quasi-Explicit Algebraic Turbulence Closures for Compressible Reacting Flows.* Ph.D. Thesis, State University of New York at Buffalo, Department of Mechanical and Aerospace Engineering, Buffalo, NY.

[38] S. SARKAR (1992), *The pressure-dilatation correlation in compressible flows.* Phys. Fluids A, 4(12), p. 2674.

[39] J. R. RISTORCELLI, G. A. BLAISDELL (1997), *Validation of a pseudo-sound theory for the pressure-dilatation in the DNS of compressible turbulence.* ICASE Report 97–53, NASA Langley Research Center, Hampton, VA. Presented at the Eleventh Turbulent Shear Flows Symposium, Sept. 8-11, 1997 Grenoble, France.

[40] J. R. RISTORCELLI (1993), *A representation for the turbulent mass flux contribution to Reynolds-stress and two-equation closure for compressible turbulence.* ICASE Report 93–88, NASA CR 191569, NASA Langley Research Center, Hampton, VA.

[41] G. A. BLAISDELL, N. N. MANSOUR, W. C. REYNOLDS (1993), *Compressibility effects on the growth and structure of homogeneous turbulent shear flow.* J. Fluid Mech., 256, p. 443.

[42] G. N. COLEMAN, P. BRADSHAW, P. G. HUANG (1995), *Compressible turbulent channel flows DNS results and modelling.* J. Fluid Mech., 305, p. 185.

[43] A. J. M. SPENCER (1971), *Theory of Invariants,* Continuum Physics, v. 1, pp. 240–352. Academic Press.

[44] G. S. SETTLES, L. J. DODSON (1993), *Hypersonic turbulent boundary-layer and free shear database.* NASA Contractor Report 177610, NASA Ames Research Center, Moffet Field, CA.

[45] P. J. COLUCCI (1997), *Large Eddy Simulation of Turbulent Reacting Flows: Stochastic Representation of the Subgrid Scale Scalar Fluctuations.* Ph.D. Thesis, State University of New York at Buffalo, Department of Mechanical and Aerospace Engineering, Buffalo, NY.

[46] D. GOTTLIEB, E. TURKEL (1976), *Dissipative two-four methods for time dependent problems.* Math. Comp., 30(136), p. 703.

[47] R. W. MACCORMACK (1969), *The effect of viscosity in hypervelocity impact catering.* AIAA Paper 69-354.

[48] R. W. MACCORMACK, B. S. BALDWIN (1975), *A numerical method for solving the Navier-Stokes equations with application to shock-boundary layer interaction.* AIAA Paper 75-1.

[49] J. P. DRUMMOND (1988), *Two-dimensional numerical simulation of a supersonic, chemically reacting mixing layer.* NASA TM 4055, NASA Langley Research Center, Hampton, VA.

[50] D. PAPAMOSCHOU, A. ROSHKO (1988), *The compressible turbulent shear layer: An experimental study.*

J. Fluid Mech., 197, p. 453.

[51] S. THANGAM, Y. ZHOU, J. R. RISTORCELLI (1996), *Analysis of compressible mixing layers using dilatational covariances model.* NASA TM 111865.

[52] S. THANGAM, Y. ZHOU, J. R. RISTORCELLI (1997), *Development and application of a dilatational covariances model for compressible jets and shear layers.* Reno, NV. AIAA Aerospace Sciences Meeting.

[53] G. S. ELLIOTT, M. SAMIMY (1990), *Compressibility effects in free shear layers.* Phys. Fluids A., 7(2), p. 1231.

[54] S. G. GOEBEL, J. C. DUTTON (1991), *Experimental study of compressible turbulent mixing layers.* AIAA J., 29(4), p. 538.

[55] K. R. SREENIVASAN (1995), *The energy dissipation in turbulent shear flows.* In *Developments in Fluid Mechanics and Aerospace Sciences*, S. M. Deshpande, A. Prabhu, K. R. Sreenivasan, P. R. Viswanath, editors. pp. 159–193, Interline Publishers.

[56] D. C. FOURGUETTE, M. G. MUNGAL, R. S. BARLOW, R. W. DIBBLE (1991), *Concentration measurements in a supersonic shear layer.* AIAA Paper 91-0627.

[57] N. T. CLEMENS, M. G. MUNGAL (1992), *Two- and three-dimensional effects in the supersonic mixing layer.* AIAA J., 30(4), p. 973.

[58] D. W. BOGDANOFF (1983), *Compressibility effects in turbulent shear layers.* AIAA J., 21(6), p. 926.

[59] M. R. GRUBER, N. L. MESSERSMITH, J. C. DUTTON (1992), *Three-dimensional velocity measurements in a turbulent, compressible mixing layer.* AIAA Paper 92-3544.

[60] G. S. ELLIOTT, M. SAMIMY (1990), *Compressibility effects in free shear layers.* AIAA Paper 90-0705.

[61] J. W. NAUGHTON, L. N. CATTAFESTA, G. S. SETTLES (1993), *Experiments on the enhancement of compressible mixing via streamwise turbulence, Part II - Vortex strength assessment and seed particle dynamics.* AIAA Paper 93-0742.

[62] S. J. KLINE, B. J. CANTWELL, G. M. LILLEY (1982). In S. J. Kline, B. J. Cantwell, G. M. Lilley, editors, *1980-1981 AFOSR-HTTM-Stanford Conference*, pp. 368–380, Stanford University Press, Stanford, CA.

[63] M. M. ROGERS, P. MOIN, W. C. REYNOLDS (1986), *The structure and modeling of the hydrodynamic and passive scalar fields in homogeneous turbulent shear flow.* Department of Mechanical Engineering TF-25, Stanford University, Stanford, CA.

[64] U. SCHUMANN (1977), *Realizability of Reynolds stress turbulence models.* Phys. Fluids, 20, p. 721.

[65] T.-H. SHIH, A. SHABBIR (1994), *Methods of ensuring realizability for non-realizable second order closures.* ICOMP 94–14, NASA Lewis Research Center, Cleveland, OH. Also available as NASA TM 106681.

Appendix A. The Poisson equation for the fluctuating pressure is obtained by taking the divergence of the Navier-Stokes equations. Both instantaneous and averaged forms of these equations are necessary in the derivation. The subtraction of the mean equations from the instantaneous equations and simple term manipulations involving the continuity relation provide the desired Poisson equation [5]:

$$\frac{\partial^2 p'}{\partial x_i^2} = \frac{\partial^2 \rho'}{\partial t^2} - \frac{\partial^2}{\partial x_i x_j} \left[\rho' \langle u_i \rangle \langle u_j \rangle + \rho u_i'' u_j'' + \rho u_i'' \langle u_j \rangle + \rho \langle u_i \rangle u_j'' - \overline{\rho} \langle u_i'' u_j'' \rangle \right] +$$

(80)
$$\frac{4}{3} \frac{\partial^2}{\partial x_i^2} \left[\frac{\mu}{Re} \frac{\partial u_k''}{\partial x_k} \right]$$

The solution for the fluctuating pressure can be determined by using Green's functions or Fourier transforms. With respect to the incompressible counterpart, the compressible Poisson equation is severely complicated. An equivalent form which resembles more to the incompressible equation can be obtained as:

$$\frac{\partial^2 p'}{\partial x_i^2} = \frac{\partial^2 \rho'}{\partial t^2} - 2 \frac{\partial^2}{\partial x_i x_j} \rho' \langle u_i \rangle u_j'' - \frac{\partial^2}{\partial x_i x_j} \left[\rho u_i'' u_j'' - \overline{\rho} \langle u_i'' u_j'' \rangle \right] - 2 \frac{\partial^2}{\partial x_i x_j} \overline{\rho} \langle u_i \rangle u_j'' +$$

(81)
$$\frac{4}{3} \frac{\partial^2}{\partial x_i^2} \left[\frac{\mu}{Re} \frac{\partial u_k''}{\partial x_k} \right]$$

The last term on the right hand side (RHS) converts, when the fluctuating pressure solution is used to determine the pressure-strain correlation, into a viscous interaction tensor whose trace is equal to the dilatational dissipation. In the absence of walls this term can be omitted in high Reynolds number flows. The acoustic term (the first term on the RHS) is difficult to be taken into account in the present analysis. If it is assumed that the pressure fluctuations are caused by turbulence only then this term is negligible. The condition $\rho'/\overline{\rho} \ll 1$ allows the neglect of the second term on the RHS. The remaining terms are the return-to-isotropy and the rapid part for which known modeling principles can be applied in the limit of low convective Mach numbers.

Appendix B. It well known that for linear pressure strain forms it is impossible to satisfy realizability conditions – the requirement that the eigenvalues of the Reynolds stress tensor remain positive. Satisfying realizability is a very practical computationally stabilizing requirement. Our experience with computations in complex flows indicates that realizability is very useful. The model is now made (weakly) realizable following methods suggested by Schumann [64] and Lumley [34] and detailed by Shih and Shabbir [65]. Let $F = 1 + 27III/8 + 9II/4$ is a parameter involving the second invariant $II = -\frac{1}{2} a_{ij} a_{ji}$ and third invariant $III = -\frac{1}{3} a_{ij} a_{jk} a_{ki}$ of the Reynolds stress anisotropy tensor. Then the following asymptotic behavior for the pressure strain-model ensures that realizability is satisfied:

$$\mathcal{A}_{ee} - \frac{2}{3} \overline{\rho} \, \overline{\epsilon} = C F^a \quad \text{as } F \to 0$$

(82)
$$\frac{\partial \langle u_p \rangle}{\partial x_q} \mathcal{I}_{peqe} \to 0 \quad \text{as } F \to 0$$

where the index e indicates that the relations are written in the principal axes of $\langle u_i'' u_j'' \rangle$. The computational form of the model with the additional parameters necessary to enforce realizability so necessary for computational stability is

$$\Pi_{ij}^\star - \overline{\rho} \, \epsilon_{ij}^\star = -C_1 \overline{\rho} \, \overline{\epsilon} a_{ij} A_r F^{\alpha_r} + \overline{\rho} \langle k \rangle \left[\left(\frac{4}{5} + \frac{2}{5} d_1 \right) S_{ij}^\star(\langle u \rangle) + \right.$$

31

$$[1 - C_3 + 2d_2]\left[a_{ip}S^{\star}_{pj}(\langle u\rangle) + S^{\star}_{ip}(\langle u\rangle)a_{pj} - \frac{2}{3}S^{\star}_{pq}(\langle u\rangle)a_{pq}\delta_{ij}\right] -$$

(83)
$$[1 - C_4 - 2d_2][a_{ip}\Omega_{pj}(\langle u\rangle) - \Omega_{ip}(\langle u\rangle)a_{pj}] + \frac{4}{3}d_2 S_{pp}(\langle u\rangle)a_{ij}\bigg] B_r F^{\beta_r}$$

with $C_3 = (5 - 9C_2)/11$ and $C_4 = (1 + 7C_2)/11$. The value for the constant C_2 will be the same as in the incompressible model to preserve consistency in the zero Mach number limit, that is $C_2 = 0.45$. The parameters are $\alpha_r = 0.1$, $\beta_r = 0.5$, $A_r = \min(F^{-\alpha_r},\ 0.1^{-\alpha_r})$ and $B_r = \min(F^{-\beta_r},\ 0.1^{-\beta_r})$.

Using this modified form of the pressure-strain model the ARSM coefficients become: $b_1 = \frac{4}{3} - B_r F^{\beta_r}(\frac{4}{5} + \frac{2}{5}d_1)$, $b_2 = \frac{1}{\bar{\rho}^2}\frac{2}{3}\tau_u\nu_0$, $b_3 = 1 - B_r F^{\beta_r}(1 - C_3 + 2d_2)$, $b_4 = 1 - B_r F^{\beta_r}(1 - C_4 - 2d_2)$, and

(84)
$$g = \left[A_r F^{\alpha_r} C_1 \frac{\overline{\epsilon}}{\overline{\epsilon}_s} + C_{\epsilon_2} - 2 + (2 - C_{\epsilon_1})\frac{P}{\overline{\rho}\ \overline{\epsilon}_s} + \frac{\tau}{\sigma}\frac{D\sigma}{Dt} + \right.$$
$$\left. \frac{2\tau}{3}(1 - 2d_2 B_r F^{\beta_r})S_{pp}(\langle u\rangle) + 2\frac{\mathcal{M} + \overline{p'd} - \overline{\rho}\ \overline{\epsilon}_c}{\overline{\rho}\ \overline{\epsilon}_s}\right]^{-1}.$$
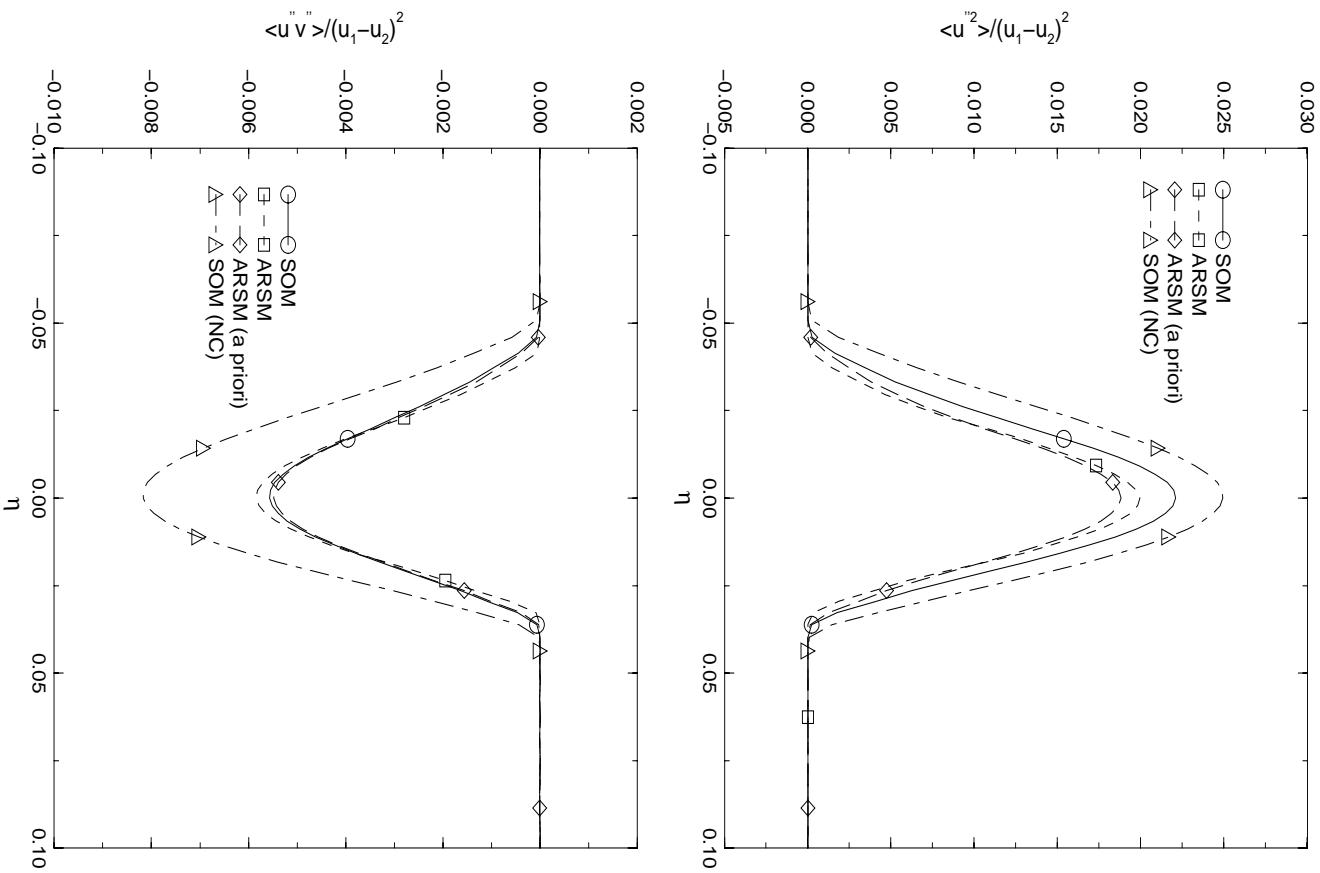
FIG. 1. *Comparisons between ARSM and SOM calculations for the mixing layer,* $M_c = 1.07$; *Top: streamwise normal Reynolds stress; Bottom: Reynolds shear stress.* $[\alpha = 1.2]$
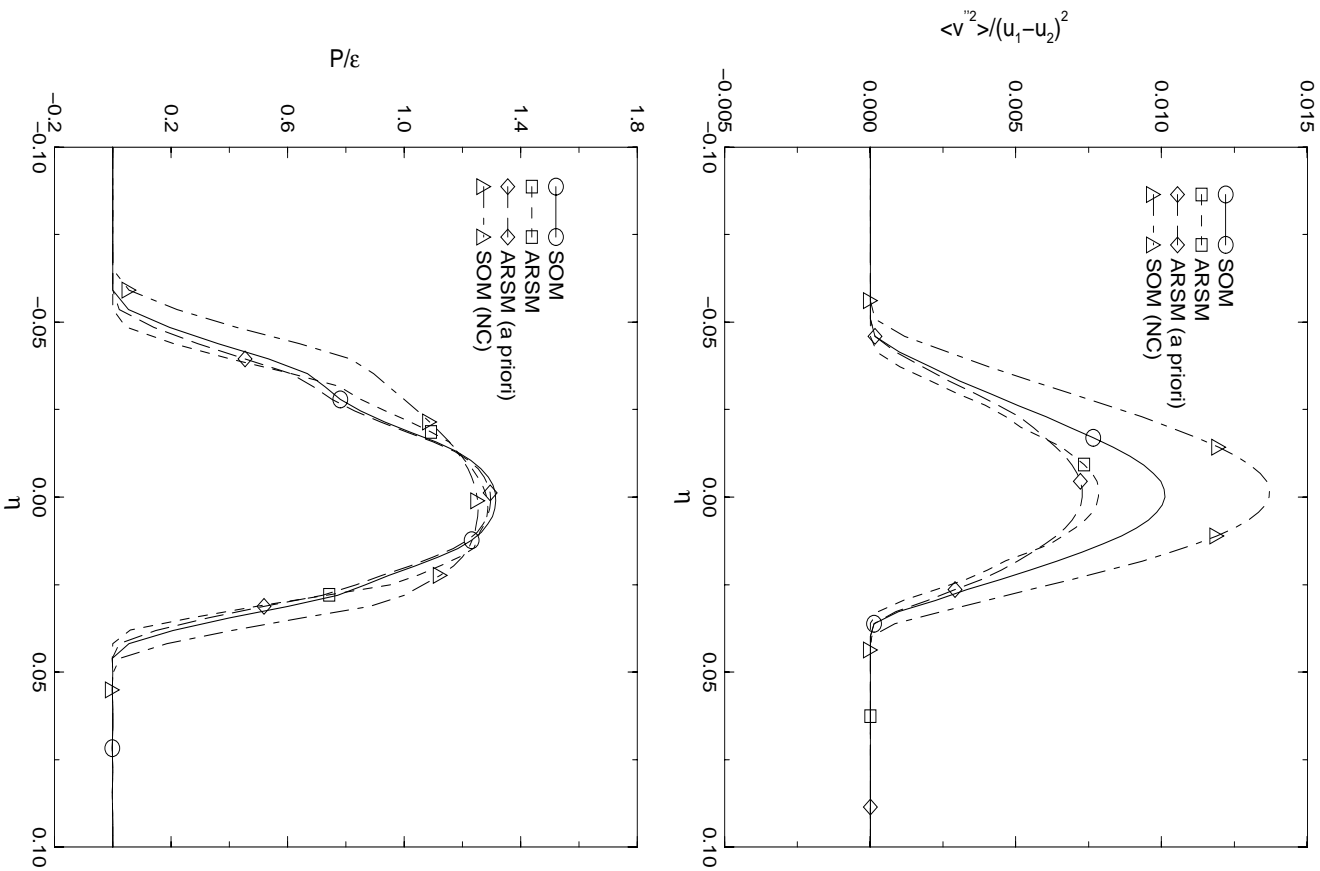
33

FIG. 2. *Comparisons between ARSM and SOM calculations for the mixing layer;* $M_c = 1.07$; *Top: crosstream normal Reynolds stress; Bottom: turbulent kinetic energy production over dissipation.* [$\alpha = 1.2$]
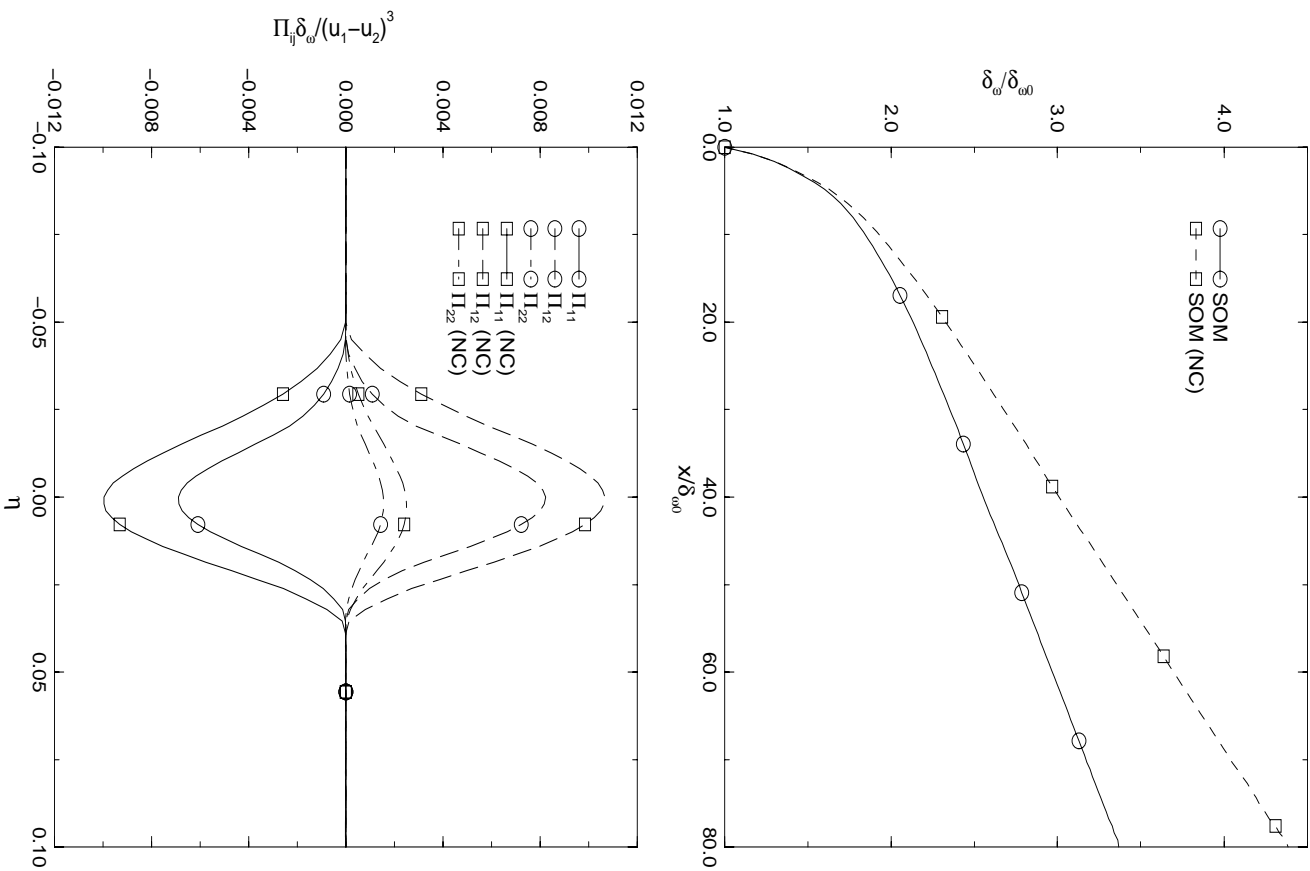
34

FIG. 3. *Influence of the compressibility correction in SOM calculations for the mixing layer, $M_c = 1.07$; Top: the vorticity thickness; Bottom: components of the pressure-strain tensor. [$\alpha = 1.2$]*
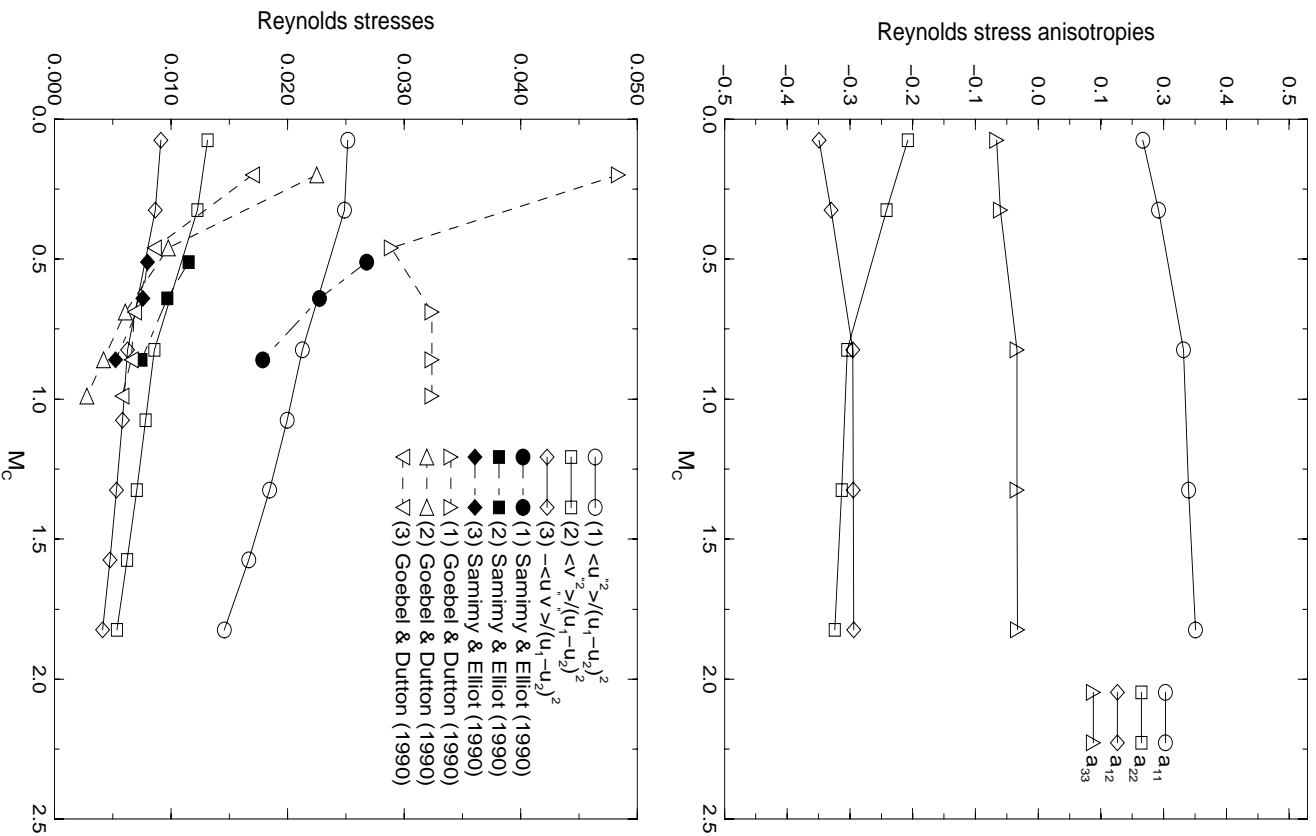
Fig. 4. *Variation with convective Mach number in the mixing layer; Top: centerline Reynolds stress anisotropies; Bottom: centerline Reynolds stresses.* [α = 1.2]

36
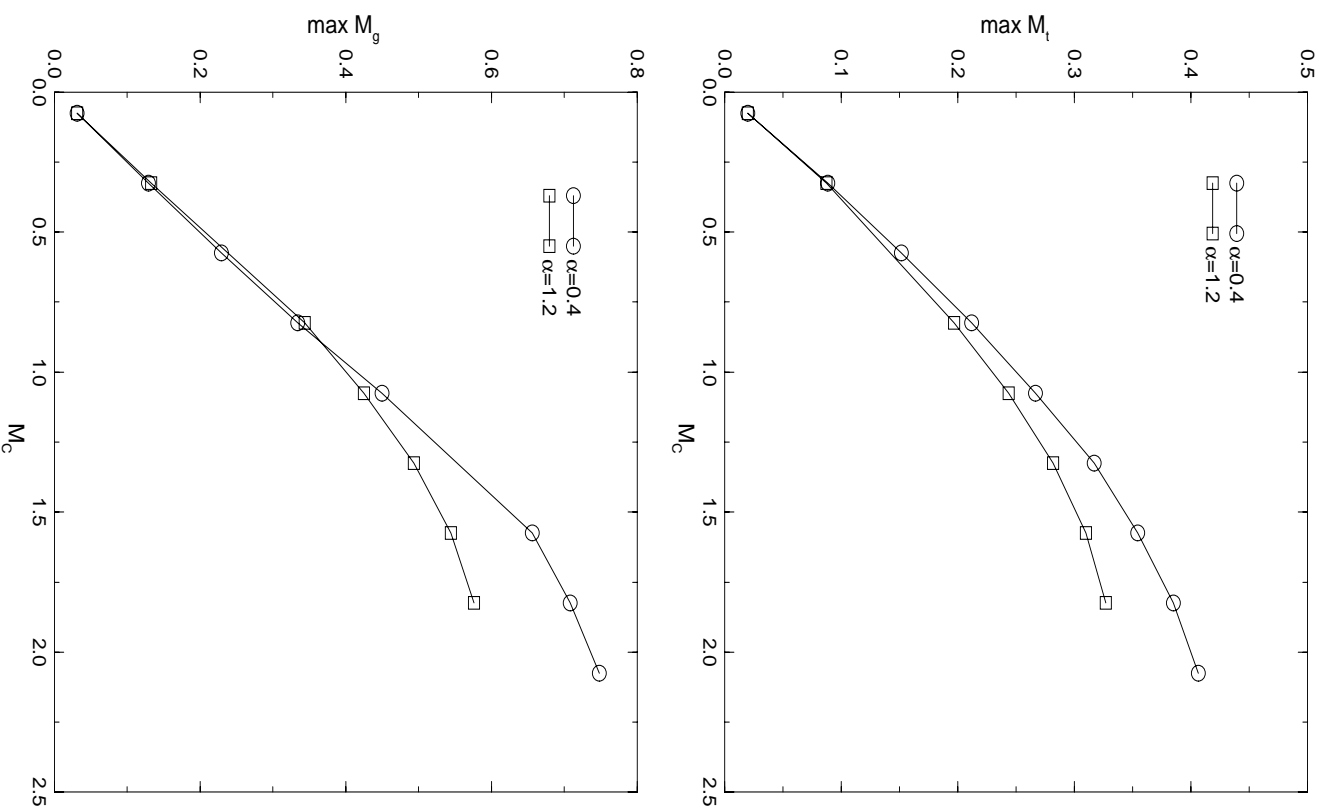
FIG. 5. *Variation with convective Mach number in the mixing layer; Top: maximum turbulent Mach number; Bottom: maximum gradient Mach number.*
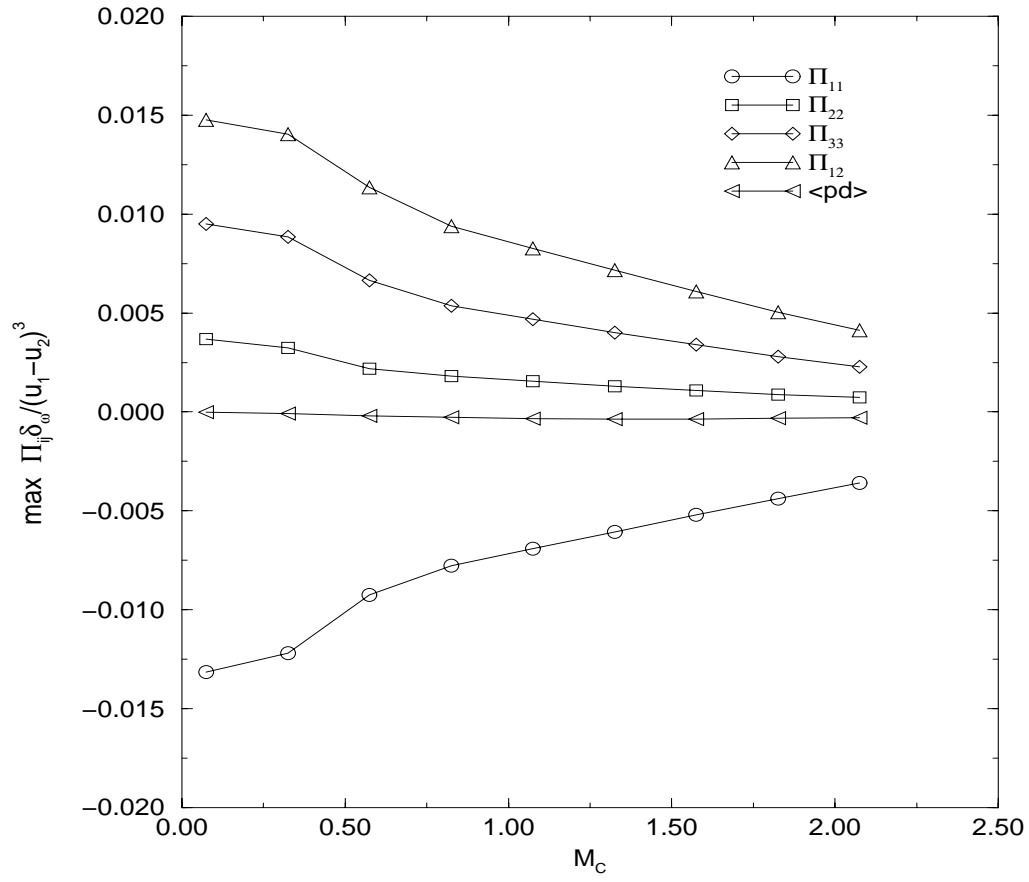
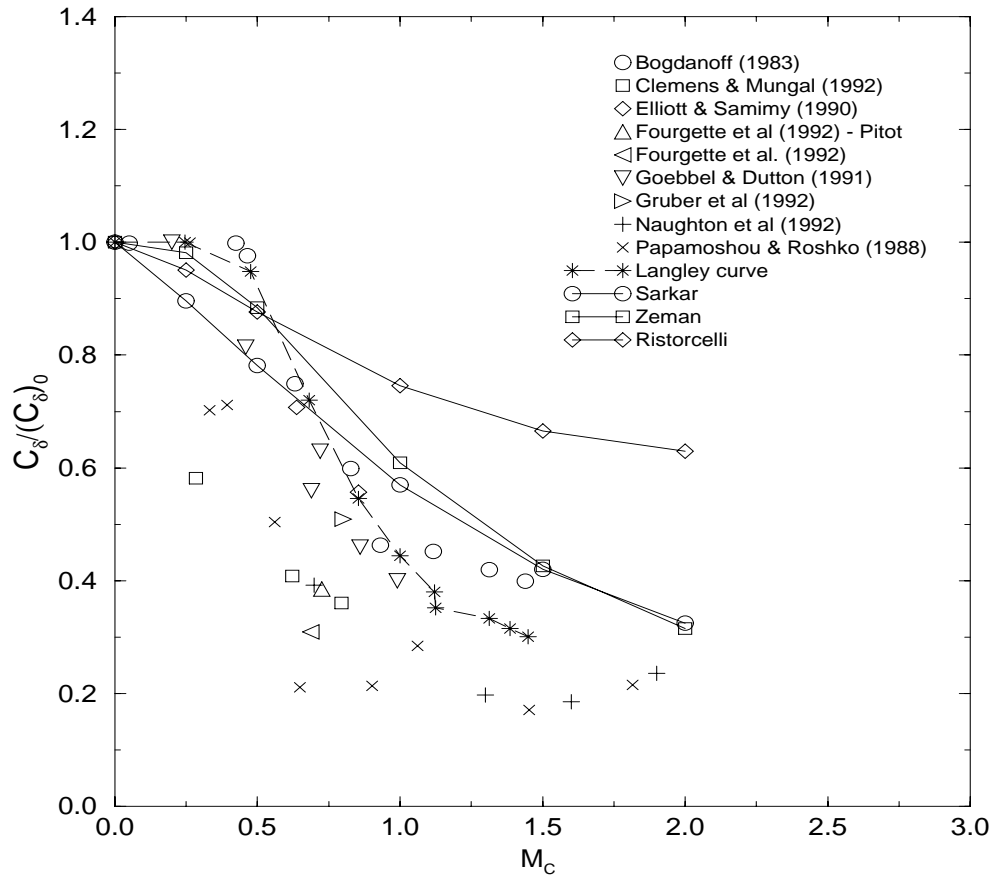FIG. 6. *Variation with convective Mach number for the mixing layer; the pressure-strain tensor.* $[\alpha = 1.2]$

FIG. 7. *Effect of compressibility on normalized thickness growth rate, $k - \epsilon$ calculations of a mixing layer.[$\alpha = 2$]*
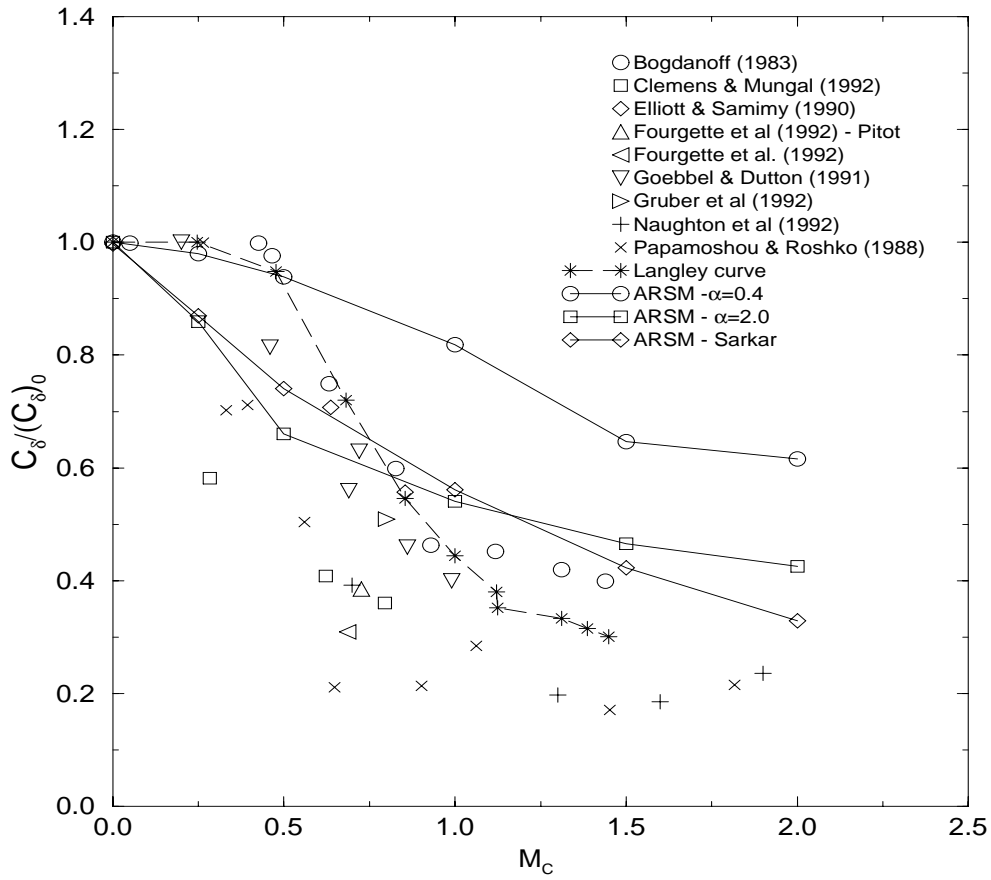
FIG. 8. *Effect of compressibility on normalized thickness growth rate, ARSM calculations of a mixing layer.*